Science of the Total Environment 839 (2022) 156302

Contents lists available at ScienceDirect

Science of the Total Environment

journal homepage: www.elsevier.com/locate/scitotenv

Determination of accurate baseline representation for three Central Iowa watersheds within a HAWQS-based SWAT analyses

Tássia Mattos Brighenti [a,*], Philip W. Gassman [a], Keith E. Schilling [b], Raghavan Srinivasan [c], Matt Liebman [d], Jan R. Thompson [e]

[a] Center for Agricultural and Rural Development, Iowa State University, Ames, Iowa 50011, United States
[b] Iowa Geological Survey, University of Iowa, Iowa City, Iowa 52242, United States
[c] Departments of Ecology and Conservation Biology, Biological and Agricultural Engineering, Texas A&M University, College Station, TX 77843, United States
[d] Department of Agronomy, Iowa State University, Ames, Iowa 50011, United States
[e] Department of Natural Resource Ecology and Management, Iowa State University, Ames, Iowa 50011, United States

HIGHLIGHTS

- The number of monitoring gauges is novel compared to previous SWAT applications.
- The RCN method improved the estimation rate between baseflow and surface runoff.
- The quantity and spatial variability of monitoring gauges improved model confidence.
- Statistical optimum (e.g., NS > 0.50) does not necessarily mean hydrological optimum.

GRAPHICAL ABSTRACT

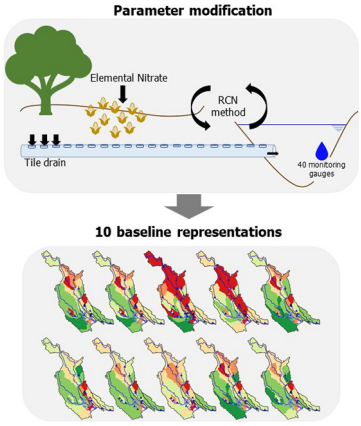

ARTICLE INFO

Editor: Ouyang Wei

Keywords:
Real system data
Soft data
Tile drainage
Nitrate
Multi-site observed streamflow data
Baseflow

ABSTRACT

Improving food systems to address food insecurity and minimize environmental impacts is still a challenge in the 21st century. Ecohydrological models are a key tool for accurate system representation and impact measurement. We used a multi-phase testing approach to represent baseline hydrologic conditions across three agricultural basins that drain parts of north central and central Iowa, U.S.: the Des Moines River Basin (DMRB), the South Skunk River Basin (SSRB), and the North Skunk River Basin (NSRB). The Soil and Water Assessment Tool (SWAT) ecohydrological model was applied using a framework consisting of the Hydrologic and Water Quality System (HAWQS) online platform, 40 streamflow gauges, the alternative runoff curve number method, additional tile drainage and fertilizer application. In addition, ten SWAT baselines were created to analyze both the HAWQS parameters (baseline 1) and nine alternative baseline configurations (considering the framework). Most of the models achieved acceptable statistical replication of measured (close to the outlet) streamflows, with Nash-Sutcliffe (NS) values ranging up to 0.80 for baseline 9 in the DMRB and SSRB, and 0.78 for baseline 7 in the NSRB. However, water balance and other hydrologic indicators revealed that careful selection of management data and other inputs are essential for obtaining the most accurate representation of baseline conditions for the simulated stream systems. Using cumulative distribution curves as a criterion, baselines 7 to 10 showed the best fit for the SSRB and NSRB, but none of the baselines accurately

* Corresponding author.
E-mail addresses: tassiab@iastate.edu (T.M. Brighenti), pwgassma@iastate.edu (P.W. Gassman), keith-schilling@uiowa.edu (K.E. Schilling), r-srinivasan@tamu.edu (R. Srinivasan), mliebman@iastate.edu (M. Liebman), jrrt@iastate.edu (J.R. Thompson).

http://dx.doi.org/10.1016/j.scitotenv.2022.156302
Received 28 March 2022; Received in revised form 11 May 2022; Accepted 24 May 2022
Available online 28 May 2022
0048-9697/© 2022 Published by Elsevier B.V.

represented 20% of low flows for the DMRB. Analysis of snowmelt and growing season periods showed that baselines 3 and 4 resulted in poor simulations across all three basins using four common statistical measures (NS, KGE, Pbias, and R^2), and that baseline 9 was characterized by the most satisfactory statistical results, followed by baselines 5, 7 and 1.

1. Introduction

One of the critically important challenges of the 21st century is the improvement of food systems, which is essential for mitigating climate change pressures, achieving sustainability, and fostering human development. Deforestation, reduction of biodiversity, degradation of soils and water, and depletion of freshwater through the use of irrigation are some of the environmental costs linked to food system activities (Béné et al., 2019; Hunt et al., 2019; Prokopy et al., 2020; Stone et al., 2021). The "Corn Belt" region is an important agricultural area in the central United States and contains some of the most productive agricultural lands in the world (Schilling et al., 2019). However, extensive land alterations have generated well-known environmental problems in the region. For example, as much as 95–99% of the original natural landscape composed of wetlands concentrated in specific western Corn Belt subregions has been lost due to surface and subsurface tile drainage (Miller et al., 2009). This transformation has enhanced crop production but has also exacerbated excess loss of nitrate (Sprague et al., 2011; Gassman et al., 2017a; Jones et al., 2018) and phosphorus (Kleinman et al., 2015), resulting in high in-stream nutrient concentrations and contributing to the seasonal oxygen-depleted hypoxic zone in the northern Gulf of Mexico (Gassman et al., 2017a; Wright and Wimberly, 2013; Jones et al., 2018). Dense urban areas in the Corn Belt region are also noted for their negative environmental impacts, due to intensive energy use, increased global greenhouse gas emissions, elevated temperatures, high levels of water consumption and wastewater production, and pollution of air, land and water (Stone et al., 2021; Thompson et al., 2021). However, urban and peri-urban agriculture can play an essential role in environmental sustainability. Urban farms, for example, can help reduce urban heat island effects, mitigate urban stormwater impacts, and lower the energy embodied in food transportation (Ackerman et al., 2014). Therefore, there has been an increasing interest in research focused on developing sustainable urban food production systems; e.g., the Iowa urban food, energy and water systems ("Iowa UrbanFEWS") nexus described by Thompson et al. (2021).

Ecohydrological models are core components within FEWS modeling efforts (Thompson et al., 2021; Kling et al., 2017; Dai et al., 2018; Schull et al., 2020; McCallum et al., 2020), and are essential for simulating water circulation and pollutant transport in dynamic landscapes. Determining optimal configuration strategies for such models is important to evaluate the hydrologic and water quality impacts of changes in land use. However, establishing reliable configurations can be approached in multiple distinct ways and there is no single procedure universally accepted in the literature (Arnold et al., 2015; Moriasi and Wilson, 2012). According to Andréassian et al. (2012); Arnold et al. (2015), Beven (2019) and Seibert and McDonnell (2002), an important initial component of applying ecohydrological models (which is sometimes ignored by modelers) is the evaluation of known infrastructure (e.g., tile drain locations), agreement with known hydrologic balance, reasonability of parameters values based on physical characteristics of the simulated system, and other 'real system data' (sometimes referred to as "soft data"; e.g., see Arnold et al., 2015, Seibert and McDonnell, 2002). This process knowledge can be incorporated into the model by manual calibration procedures, which combine expert knowledge, literature information or other reliable sources of information (e.g., detailed management operations for crops, detailed spatial representation of best management practices) with the intention of increasing the efficacy and accuracy of parameter estimations for initial watershed simulations and subsequent automatic calibration.

The Soil and Water Assessment Tool (SWAT) ecohydrological model (Arnold et al., 1998, 2012) incorporates over three decades of development that is represented by several major versions (Bieger et al., 2017; Gassman and Wang, 2015). SWAT has been used worldwide to evaluate an extensive suite of climatic, hydrologic and/or environmental problems across a wide range of watershed scales and conditions as documented in a variety of reviews (e.g., Akoko et al., 2021; Bressiani et al., 2015; Brighenti et al., 2019; Gassman et al., 2007, 2022; Tan et al., 2019, 2020). The Corn Belt region has been targeted by dozens of SWAT studies, that have encompassed a wide range of topics (CARD, 2022). However, little attention has been paid to date to the role of determining optimal initial SWAT setup strategies within the context of Corn Belt region applications. Thus, this study seeks to inform that gap in support of hydrologic and water quality assessments for the Iowa UrbanFEWS project (Thompson et al., 2021).

The simulated stream systems represented in this study, as part of the UrbanFEWS integrated modeling project, are composed of the Des Moines River Basin (DMRB), the North Skunk River Basin (NSRB) and the South Skunk River Basin (SSRB), which drain to and through the Des Moines-West Des Moines, IA Metropolitan Statistical Area (DMMSA; US OMB, 2018), Iowa, USA (Fig. 1). The SWAT model applications have been implemented using a framework consisting of the Hydrologic and Water Quality System (HAWQS) on-line platform (HAWQS, 2020). The HAWQS platform supports rapid construction of SWAT models for watersheds in the contiguous USA using subwatersheds based on 12-, 10- or 8-digit hydrologic unit watersheds (as described by USGS, 2013, 2022) and pre-loaded climate, land use, management and other data. The use of HAWQS represents the first phase of SWAT model development within the larger project, which was implemented using a 12-digit discretization (Chen et al., 2021).

Portions of the simulated watersheds for this study were originally dominated by wet prairies and wetlands characterized by poorly drained soils; agricultural production would be problematic for these areas without changes in drainage (Ikenberry et al., 2017; Schilling et al., 2019). A common drainage practice is the implementation of subsurface tile drains (Moriasi et al., 2012; Gassman et al., 2017a, 2017b; Schilling et al., 2019), which allow crop production and improve crop yields in poorly drained soils by increasing the time available for planting and harvesting operations. Tile drains result in significant impacts on both watershed hydrology (by altering baseflow proportion) and water quality (by carrying excess nutrients directly to waterways). Therefore, detailed geographical information and accurate model parameters are crucial to produce reliable tile drain effects within ecohydrological model simulation (Moriasi et al., 2013; Valayamkunnath et al., 2020). Accurate accounting of nitrogen (N) fertilizer application rates is equally important for model simulations because N is one of the most important nutrients used to enhance corn productivity (Gassman et al., 2017a; Yang et al., 2016) and contributes to serious water quality impairment across the study area (Schilling and Wolter, 2009; Gassman et al., 2017a). Corn growth and yield could be negatively affected by inadequate N fertilizer amounts in model development, causing misleading water balance simulations. Spatially distributed models such as SWAT have the advantage of providing detailed ecohydrological information across a simulated watershed. However, the use of distributed models is justified only if their results can be used with some confidence (Moussa et al., 2007). The most common way to measure model efficacy is against measured streamflow data, and this is associated with the fact that these data are often available and the process itself is the driving force for other processes, for example, suspended sediment and nutrient transport. This is usually done based on comparisons with one monitoring gauge at the basin outlet. However, this level of testing may not provide a completely accurate hydrologic assessment, especially for large basins, and thus the calibration process ends up focusing on refining the performance indices rather than improving the representation of actual processes in these

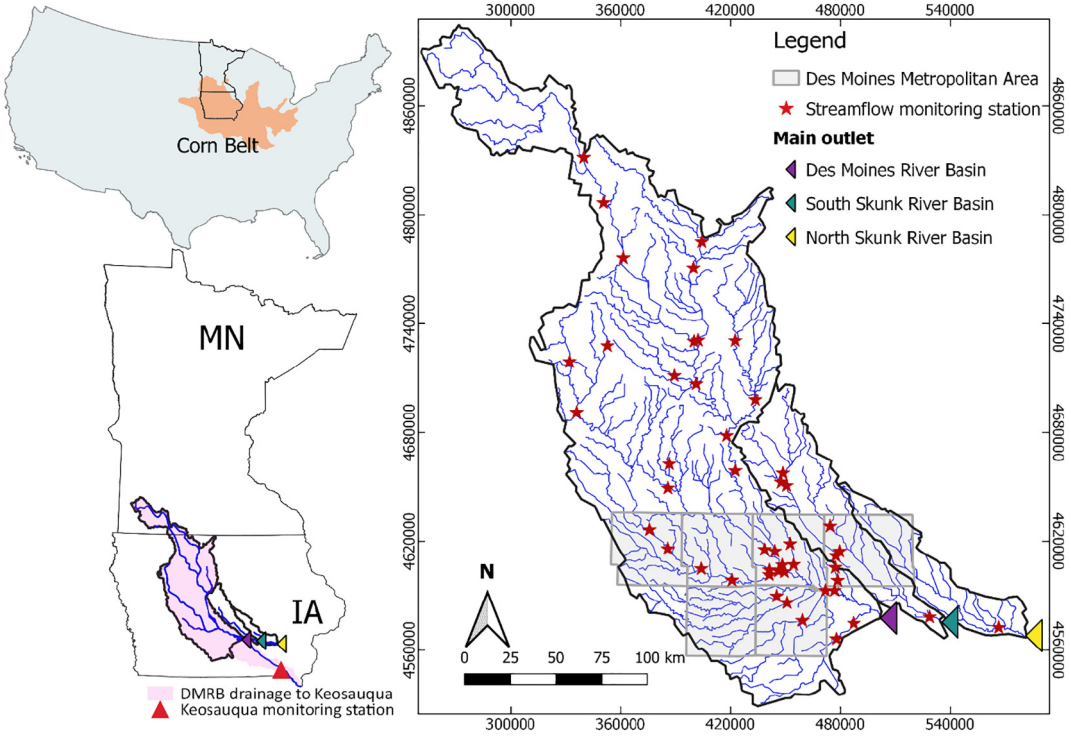

Fig. 1. Study area location in Minnesota (MN) and Iowa (IA), USA, and streamflow monitoring gauge distribution for the Des Moines, South Skunk, and North Skunk River Basins. The DMRB drainage to Keosauqua and monitoring station (Table 3) are also shown (bottom left).

models (Acero Triana et al., 2019). Therefore, the use of multi-site observed data is crucial to obtaining the best representation of processes and overall simulation results.

This study offers important insights for representation of individual processes that can influence the water cycle at a watershed scale. This was accomplished via a multi-phase testing approach for SWAT model simulations, which were performed as a function of different baseline configurations. The baselines were not calibrated or validated, incorporated either HAWQS defaults for management and/or alternative management, and also reflect alternative runoff curve number (RCN) methods (Neitsch et al., 2011; Williams et al., 2012). The specific objectives of this study were to: (1) identify the importance of accurate representation of tile drain locations, density and model input parameters, (2) quantify the effects of different amounts of N fertilizer applications on corn biomass production and grain yields, (3) analyze the impacts of different RCN surface runoff methods on the water balance, (4) identify accurate baseflow performance, and (5) evaluate the spatial efficiency of SWAT model simulations based on statistical and graphical measures.

2. Materials and methods

2.1. Study area

The DMRB (31,892.4 km^2), SSRB (4593.5 km^2) and NSRB (2259.6 km^2) are the three basins that comprise the DMMSA drainage system, which collectively drain a small portion of southern Minnesota and much of north central and central Iowa (Fig. 1). Land use in the study area (Table 1) is predominantly agricultural, with soybean and corn fields representing together 70%, 71%, and 61% of land use in the DMRB, SSRB, and NSRB, respectively. The major soil types are: Udolls - more or less freely drained soils classified as Mollisols, as well as Aquolls - wet Mollisols, and Udalfs – freely drained soils classified as Alfisols (USDA-NRCS, 2021; see Supplementary Material for detailed soil type and percentages for each basin). The climate is Dfa following the Köppen classification (Peel et al., 2007), represented by a humid continental climate with hot summers and cold winters. Subsurface tile drains are distributed across portions of all watersheds, with especially intensive use in the middle-to-northern portions of the three basins (see Section 2.5). Landscapes managed with tile drainage represent 54%, 51% and 44% of the DMRB, SSRB and NSRB, respectively.

Long-term streamflow data are available for the entire watershed via the U.S. Geological Survey (USGS) data repository (<https://waterdata.usgs.gov/nwis>). A total of 40 monitoring gauges were selected for the study area with time series of 5 years or more of streamflow data (Fig. 1), within a simulation time-span from 2001 to 2018; 31, 4, and 3 stations have 18, 4 and 3 years of monitoring data available, respectively, and two other stations have either 16 or 10 years of monitoring data. Data were downloaded at a daily time step and subsequently aggregated to a monthly time step. The gauges are distributed across the three basins, with a concentration of stations in the DMMSA. A total of 32, 7, and 1 station are located in the DMRB, SSRB, and NSRB, respectively.

2.1.1. Multi-site studies

Evaluations of SWAT applications using multiple gauges are relatively uncommon among the thousands of studies in the existing literature (CARD, 2022). A succinct literature review was conducted to identify studies that used a multi-site approach. A total of 26 articles were identified in the SWAT literature database (CARD, 2022) searching for the word "multi-site"; 16 were relevant for this review. A second round of literature

Table 1
Land use distribution (%) across the DMRB, SSRB and NSRB study areas.

Land use	Des Moines River basin (%)	South Skunk River basin (%)	North Skunk River basin (%)
Rotation corn-soybean	56	53	51
Continuous corn	13	17	9
Continuous soybean	1	0.8	1
Hay	8	7	14
Range-grasses	5	7	12
Urban	8	9	7
Forest	5	0.02	5
Wetlands	2	1	1

investigation was performed using Google Scholar with the same "multi-site" word search, resulting in 23 additional studies. Fig. 2a shows how the total number of gauges used in this study for the DMRB and SSRB compared with the 39 previous SWAT studies that reported multi-gauge evaluations of SWAT streamflow output (see Supplementary material regarding those studies). The density of gauges per km^2 was also assessed for each study (Fig. 2b). A total of 47 data points is shown in both figures because two or more simulated basins were reported in some studies.

The seven gauges incorporated for the SSRB evaluations represent >81% of the total number of gauges reported in the previous 39 studies (Fig. 2a). The SSRB gauge density is >56% of the basins within a similar range of areas (900 to 9999 km^2) and 68% of the total basins (Fig. 2b). The 32 gauges used for the DMRB evaluations exceed the cumulative total gauges reported in all of the previous 39 studies (Fig. 2a). On a density basis, the total DMRB gauges is higher than all basins of a similar areal extent (10,000 to 99,999 km^2) and >66% of the total basins (Fig. 2b). There are additional studies that used larger sets of gauges, including hundreds of gauges for the European continent (Abbaspour et al., 2015) and dozens of gauges for the Missouri River Basin (Daggupati et al., 2016) and Mekong River Basin (Rossi et al., 2009). Chen et al. (2020) also reviewed 41 Upper Mississippi River Basin SWAT studies, of which 15 used a multi-site approach (with a maximum number of 13 gauges). Overall, the number of gauges used in this study is relatively novel compared to previous SWAT applications.

2.2. Modeling system

Key data flows and simulation steps constructed for the modeling system are shown in Fig. 3. The HAWQS platform served as the primary source of land use, soil, topographic, hydrography (subwatershed boundaries and streams) and weather data for the modeling system. Importantly, HAWQS was used in this study to provide an initial repository of required data layers for the DMRB, SSRB and NSRB SWAT models. Some of the current HAWQS data layers will ultimately be replaced by enhanced and/or refined counterpart data layers (e.g., the soil layer data as discussed in Section 2.4) in future Iowa UrbanFEWS research efforts.

Ten different baseline configurations (described in Section 2.7) were simulated to provide a basis for evaluating different combinations of key input data and RCN methods (Fig. 3). These baseline configurations included alternative representations of the areal extent of subsurface tile drainage, the distribution of nitrogen fertilizer rates, and the effects of two different RCN equations described in Section 2.3. The alternative tile drainage and nitrogen fertilizer rates were explored due to anomalies encountered in the HAWQS management data assumptions (discussed in Section 2.6).

Each baseline was executed in SWAT independently for the DMRB, SSRB and NSRB systems (Fig. 3). Outputs generated by the model include streamflow, water quality (i.e., nutrients and sediment) and crop yields. Pollutant losses were not incorporated in this study but will be investigated in future research. Statistical and hydrograph evaluations of the predicted streamflow outputs were conducted using streamflows measured at the 40 gauges (Fig. 1). Predicted DMRB streamflows were analyzed using 32 gauges, the SSRB using eight gauges, and the NSRB using one gauge (Fig. 1).

Several hydrologic indicators were considered to analyze the differences between the ten baselines including total water balance, relative contributions of baseflow versus surface flow to streamflow, and comparisons between observed and simulated streamflow data. The Web-based Hydrograph Analysis Tool (WHAT) software (Lim et al., 2005) was used to separate estimated baseflow from surface runoff (via digital filter application) at the streamflow monitoring gauges closest to the DMRB, SSRB and NSRB outlets (Fig. 1). These WHAT-derived estimates were used to represent the observed baseflow and surface runoff values for this study. The accuracy of simulated streamflow was determined by statistical evaluations and graphical representations relative to measured streamflows. This combined approach - using graphical results, absolute value errors and normalized goodness-of-fit statistics - avoids the use of a single indicator which could lead to incorrect verification of the model.

2.3. SWAT model

SWAT is a continuous and physically-based ecohydrological model developed to explore the effects of climate and land management practices on water, sediment, and pollution (Arnold et al., 2012; Gassman et al., 2007, 2014). The SWAT hydrologic component is based on a soil profile water balance equation that accounts for several processes including precipitation, surface runoff, infiltration, evapotranspiration (ET), lateral flow, percolation and groundwater flow. The model simulation unit is the Hydrological Response Unity (HRU) which is defined as an area comprised of unique land cover, soil type, and management practices within a given subbasin (Neitsch et al., 2011). The Penman-Monteith equation was used to calculate potential ET and the Variable Storage method was used to simulate channel processes (Neitsch et al., 2011). Two different approaches were used to calculate surface runoff: the traditional runoff curve number (CN) method (Neitsch et al., 2011) and an alternative runoff curve number (RCN) approach (Kannan et al., 2008; Neitsch et al., 2011; Williams et al., 2012). The latter is calculated as a function of ET using a CN coefficient (CNCOEF).

The traditional CN runoff method is calculated as follows:

$$S = S_{max}\left(\frac{SW}{[SW + \ exp(w_1 - w_2 * SW)]}\right) \quad (1)$$

alternative runoff curve number (RCN) approach (USDA-NRCS, 2004) computed as a function of evapotranspiration (ET).where S is the retention parameter for a given day (mm), S_{max} is the maximum value the retention

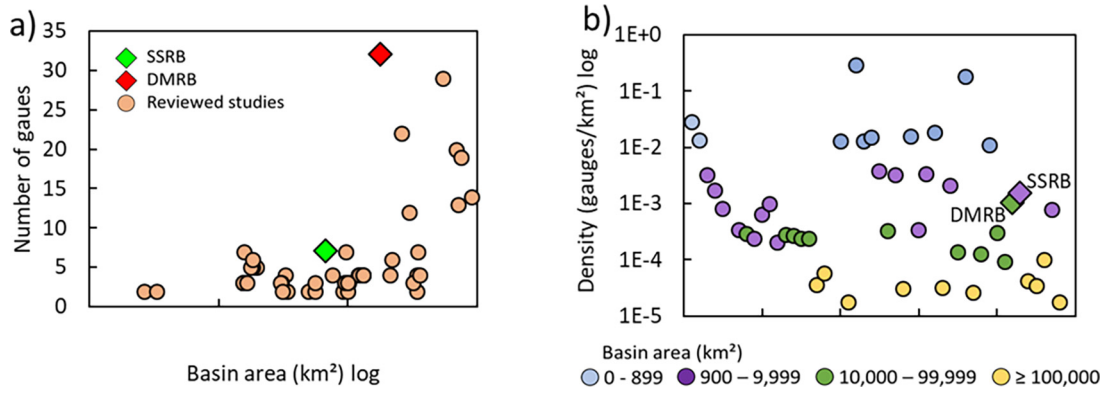

Fig. 2. a) Comparisons of total gauges and basin areas used for the DMRB and SSRB SWAT applications versus 47 cumulative gauge sites and basin areas used in 39 previous SWAT studies (Supplementary material), and b) Density of gauges for each of the 47 basins presented in Fig. 2a.

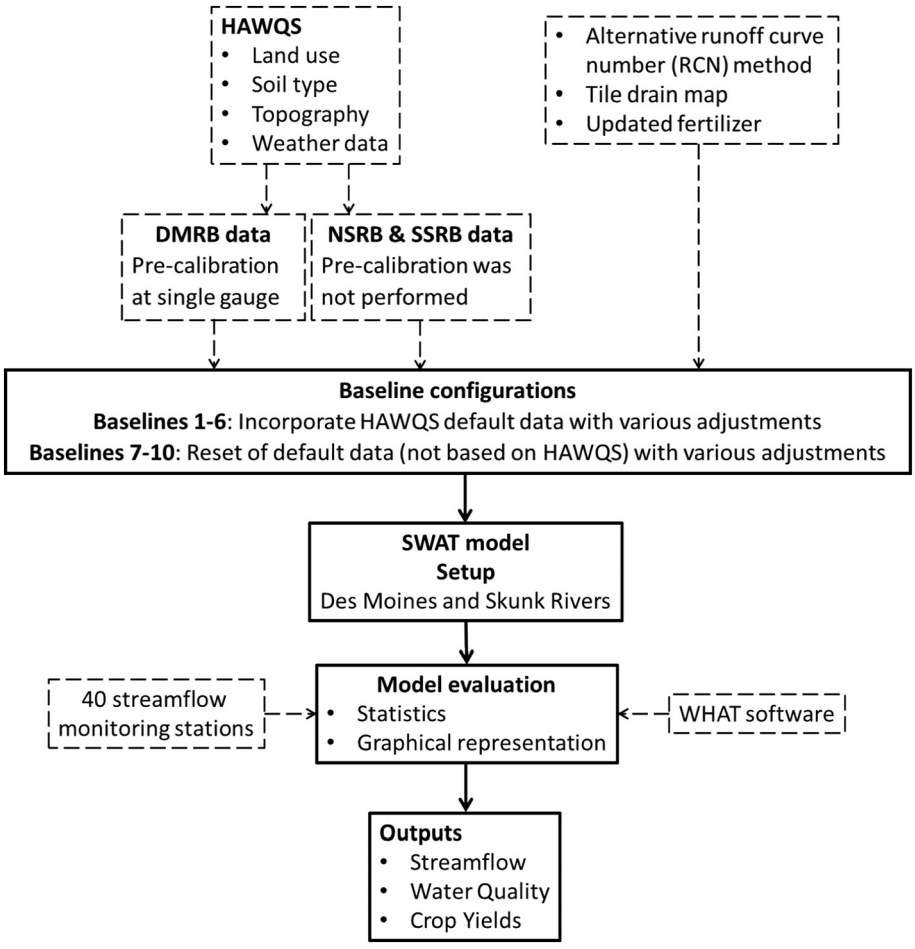

Fig. 3. Flow chart for data flows from HAWQS and other data sources which were used to create 10 different baselines simulated in SWAT for the study region in Minnesota and Iowa, USA.

parameter can reach on any given day (mm), *SW* is the soil water content of the entire profile excluding the amount of water held in the profile at wilting point (mm H2O), and w_1 and w_2 are shape coefficients.

The alternative CN method is computed with the following equation:

$$S = S_{prev} + E_0 * \ exp\left(\frac{-CNCOEF - S_{prev}}{S_{max}}\right) - R_{day} - Q_{suf} \quad (2)$$

where S_{prev} is the retention parameter for the previous day (mm), E_0 is the potential ET for the day (mm/day), *CNCOEF* is the weighting coefficient used to calculate the retention coefficient for daily CN calculations dependent on plant ET, R_{day} is the rainfall depth for the day (mm H2O), and Q_{suf} is the surface runoff (mm H2O).

SWAT can also simulate water movement through tile drains in the soil profile. Tile drainage is simulated at the HRU level and can be estimated using two different methods in SWAT: (1) an original method that accounts for tile drain depth and selected drainage parameters, and (2) a modified option that is based on the approach used in the DRAINMOD model (Skaggs et al., 2012) that incorporates drain tile spacing and other parameters (Moriasi et al., 2012, 2013). The original method was used for this study was parametrized for: tile drain depth (DDRAIN; mm), the time required to drain the soil to field capacity (TDRAIN; h), tile drain lag time (GDRAIN; h) and an impervious layer depth (DEP_IMP, mm) as described by Neitsch et al. (2011). Tile drainage occurs when the water table rises above the depth of the drains. It is important to recognize that the model will activate the tile drain equation if a positive value is entered for DDRAIN; in this case, default values of 96 h and 24 h will be activated for GDRAIN and TDRAIN, respectively. The amount of water that enters a tile drain on a given day is calculated by Eq. (3) (Neitsch et al., 2011):

$$tile_{wtr} = \frac{h_{wtbl} - h_{drain}}{h_{wtbl}} * (SW - FC) * \left(1 - \ exp\left[\frac{-24}{t_{drain}}\right]\right) \ if \ h_{wtbl} > h_{drain} \quad (3)$$

where, $tile_{wtr}$ is the amount of water removed from the layer on a given day by the tile drain (mm H2O), h_{wtbl} is the height of the water table above the impervious zone (mm), h_{drain} is the height of the tile-drain above the impervious zone (mm), *SW* is the water content of the profile on a given day (mm H2O), *FC* is the field capacity water content of the profile (mm H2O), and t_{drain} is the time required to drain the soil to the field capacity (h).

2.4. HAWQS platform and inputs

The HAWQS platform allows selection of different sources of weather data, time step of simulation (daily, monthly, or yearly), and previously described watershed spatial discretization (e.g. 8-digit, 10-digit and 12-digit). However, the topographic model, and land use and soil maps are pre-determined in current HAWQS versions 1.1 and 1.2 (Texas A&M, 2019; https://hawqs.tamu.edu/#/help) per details and sources of the datasets (Table 2). There are limitations regarding currently available data layers; for example, the coarse resolution of the Digital General Soil Map of the United States (STATSGO) (Table 2). The STATSGO map will be replaced by the more refined Soil Survey Geographic Database (SSURGO) (USDA-NRCS, 2022a, 2022b, 2022c) in future applications of the DMRB, SSRB and NSRB SWAT models. This refinement (along with other data layer revisions, e.g., climate products such as Iowa

Table 2
Description of the nature and source of datasets employed in this study.

Data	Description	Source
DEM	30 m resolution map	US Geological Survey (USGS) National Elevation Dataset
Land use map	Vector database	USGS National Land Cover Database (NLCD); Cropland Data Layers (CDL) (USGS, 2018; USDA-NASS, 2022)
Soil map	1:250,000-scale	Digital General Soil Map of the United States (STATSGO) (USDA-NRCS, 2022a, 2022b)
Weather data	Rainfall, temperature, humidity, wind speed, solar radiation	Parameter-elevation Relationships on Independent Slopes Model (PRISM) (PRISM Climate Group, 2022; Daly et al., 2008)

Table 3
Streamflow station used in HAWQS calibration process, USGS station ID, Nash-Sutcliffe and Pbias monthly statistical results, and years used in the HAWQS calibration.

Name	Des Moines River at Keosauqua, IA
USGS station ID	05490500
NS	0.70
Pbias	8.97
Calibration years	1983–2001

Environmental Mesonet <https://mesonet.agron.iastate.edu/>) can be accomplished by shifting to the forthcoming HAWQS version 2.0 (R. Srinivasan. 2022. Personal communication. Spatial Sciences Laboratory, Texas A&M AgriLife Research. College Station, TX) and/or by accessing other data sources (e.g., Iowa Geospatial Data <https://geodata.iowa.gov/>).

SWAT is presented as a partially monthly calibrated model in the HAWQS platform, in which calibration has been performed for 30% of the 8-digit watersheds (Texas A&M, 2019). The calibration is performed on the basis of both the primary default data layers (Table 2) and management inputs configured for agricultural land use. The latter includes subsurface tile drainage and nutrient application rates that are described in more detail below. In reference to our study area, HAWQS calibration was performed for the DMRB for a single USGS gauge located near Keosauqua, Iowa, which is downstream of the study area outlet (Fig. 1). The model was calibrated based on a monthly time step via the split-sample calibration/validation procedure, where calibration was performed by comparing simulated results to a minimum of five years of observed flow data. The USGS station used for streamflow calibration, final Nash-Sutcliffe (NS) and Percent Bias (Pbias) statistical coefficients, and years of calibration reported for the HAWQS calibration at Keosauqua (Fig. 1) are listed in Table 3. The calibrated parameters used for the default HAWQS simulation are presented in Appendix A. The North and South Skunk River basins are not part of the calibrated basin and have their own parameter sets (also in Appendix A; see USEPA, 2019 for more information regarding HAWQS parameters).

2.5. Tile drainage inputs

The configuration of the default HAWQS baseline models (baseline 1; Section 2.7) incorporated tile drain structures at the HRU level. However, the distribution of tile drains varied considerably between the DMRB default SWAT model and the two Skunk River SWAT models. The DMRB SWAT model included the following tile drain related parameter values: DDRAIN was set at a depth of 1420 mm for all HRUs (100% of the watershed area), while the TDRAIN (78 h) and GDRAIN (48 h) inputs were set for just 2.9% of the total area (Table 4). However, the previously described default TDRAIN and GDRAIN values of 24 h and 96 h were automatically inserted by the SWAT code for the other 97.1% of the simulated area. In contrast, tile drains were configured in the default HAWQS NSRB and SSRB SWAT models for only 0.61% and 0.1% of the total respective areas (Table 4). The same tile drain values were set by HAWQS for the two default Skunk River SWAT models: DDRAIN = 1200 mm; TDRAIN = 72 h; GDRAIN = 48 h.

Inconsistencies in the HAWQS tile drain distributions and parameter selections in the DMRB, SSRB and NSRB default SWAT models, underscored the need to develop improved tile drain inputs for all three models. Thus, an alternative tile drain distribution map was constructed for the three basins (Fig. 4) to assess the impacts of improved tile drain representation in the baseline SWAT models. The alternative tile drain layer was based on the map compiled by Valayamkunnath et al. (2020), who reported that their methodology attained 86% accuracy based on comparisons with 16,000 ground truth points across the contiguous U.S. (Fig. 4).

Insertion of the tile drain map into the SWAT models was driven by transforming map pixels (Fig. 4) into subbasin percentages. Three steps were followed to achieve the final tile drain distribution: (1) the percentage of the tile drained area for each subbasin was determined by overlapping the 12-digit subbasin shapefile and the tile drain raster file, (2) the tile drained area was then distributed among agricultural land uses in a given 12-digit subbasin, giving priority to cropland planted in soybean and corn, and (3) the DDRAIN, GDRAIN and TDRAIN parameters were set in the three SWAT models with values of 1200 mm, 48 and 24 h, respectively, based on Gassman et al. (2017b). Following creation of the maps, the percentages of cropland estimated to be managed with tile drains were 55.6% for the DMRB, 57.7% for the SSRB and 45.7% for the NSRB (Table 4).

2.6. Nitrogen fertilizer application rates

Configuration of different management operations for a simulated basin in SWAT is performed via operation management (.mgt) input files. These files contain inputs for planting, harvest, irrigation, and tillage operations, and for nutrient and pesticide applications. SWAT also computes nitrogen stress days for the associated crop, which is quantified by comparing actual and optimal plant nitrogen levels (Neitsch et al., 2011). HAWQS generates a default distribution of nitrogen fertilizer rates, on the basis of applied elemental nitrate (Table 5). The exact distribution of nitrogen application rates is impossible to determine for the study area as well as for the entire Corn Belt region. However, the lower two ranges of the HAWQS default application rates (Table 5) are well below optimal nitrogen application rates used in corn-soybean and continuous corn rotations in Iowa (ISU, 2018). Thus, an alternative distribution of nitrogen application rates was configured (Table 6), based on previous rates reported by Gassman et al. (2017a) for the Boone River Watershed (a subwatershed of the DMRB), which reflect more typical rates in the region and provide baseline comparisons with the HAWQS default rates.

Table 4
Tile drain area and percentages for each watershed before/after tile drain map implementation.

SWAT parameters	Des Moines River basin				South Skunk River basin				North Skunk River basin			
	Default HAWQS		Tile drain map		Default HAWQS		Tile drain map		Default HAWQS		Tile drain map	
	km^2	%	km^2	%	km^2	%	km^2	%	km^2	%	km^2	%
DDRAIN	31,892	100	17,727	55.6	28	0.61	2649	57.7	0.3	0.01	1033	45.7
TDRAIN	939	2.9	17,727	55.6	28	0.61	2649	57.7	0.3	0.01	1033	45.7
GDRAIN	939	2.9	17,727	55.6	28	0.61	2649	57.7	0.3	0.01	1033	45.7

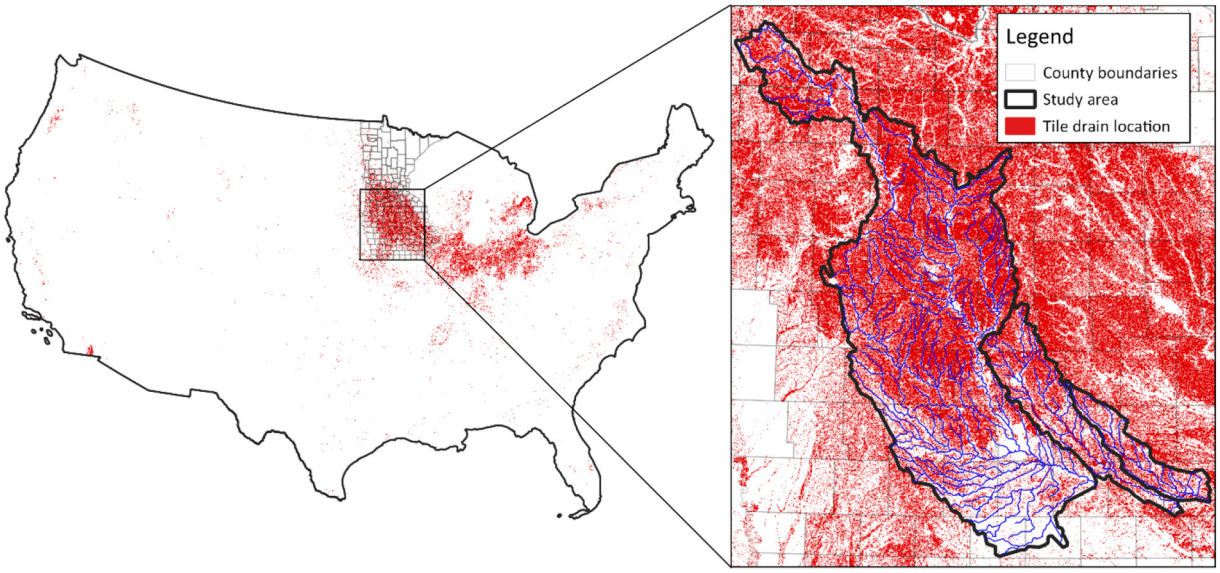

Fig. 4. Spatial distribution of tile drainage across the U.S. and for the 12-digit subbasins in the study area.
Source: Valayamkunnath et al., 2020.

2.7. Baseline simulations

Ten baseline simulations were created to analyze both the default HAWQS input parameters (baseline 1) and nine alternative baseline configurations (Table 7). The suite of ten baseline simulations were organized into two distinct subsets: (1) six baseline simulations (1 to 6) that incorporated the HAWQS default inputs and various modifications as described below, and (2) four baseline simulations (7 to 10) that were executed on the basis of an uncalibrated "reset of the initial input parameters" (not based on the HAWQS default input parameters). The return to a non-calibrated SWAT (7 to 10) was performed by re-writing the model input tables (instead of using HAWQS to generate those), which set the input parameters back to the default values described in the SWAT Theoretical Manual (Neitsch et al., 2011). These additional four baseline simulations provided further rigorous testing of SWAT due to the fact that calibration was not performed prior to the model testing phase.

The alternative baseline simulations (2 to 9) were also parameterized as a function of one or more of the following factors: (1) the addition of the previously described improved areal representation of tile drains (Fig. 4 and Table 4), (2) the revised distribution of nitrogen fertilizer application rates for corn production (Table 6), and (3) use of the previously described alternative RCN method (Eq. (2)) to calculate partitioning between surface runoff and infiltration. The change between the standard RCN method and alternative RCN method is made in the Surface Runoff component of the SWAT BASIN module (.bsn input file), where a user can choose different RCN methods. For this study, the CNCOEF (RCN) value (Eq. (2)) was fixed at 0.75 based on previous sensitivity testing reported by Schilling et al. (2019) and Gassman et al. (2017b). The period for all ten baseline simulations ranged from 2001 to 2018, each of which was preceded by a two-year warm-up period.

2.8. Statistical coefficients

Four statistical coefficients were used to assess the SWAT baseline simulation results: Coefficient of determination (R^2), Nash-Sutcliffe modeling efficiency (NS), Percent Bias (Pbias) and Kling-Gupta Efficiency (KGE). The R^2 is a statistical measure for a regression model that explains the proportion of variance in the dependent variable that is predictable from the independent variable (Moriasi et al., 2015). The NS is the most widely used objective function in hydrological modeling including SWAT model applications (e.g., Gassman et al., 2007, 2014; Tan et al., 2019). It is a normalized statistic that determines the relative magnitude of residual variance compared to measured data variance, where 1 is a perfect simulation, zero represents balance accuracy, and observations below zero represent unacceptable model performance (Moriasi et al., 2007). The Pbias evaluates the trend for an average of the simulated values in relation to observed values, and can be linked to how well the model simulates water volume (Moriasi et al., 2007).The KGE (Gupta et al., 2009) is a decomposition of NS into three components: *alpha* (measure of relative variability in the simulated and observed values), *beta* (bias normalized by the standard deviation in the observed values), and *r* (correlation coefficient). This allows unequal weighting of the three components to emphasize certain areas of the aggregated function tradeoff space. Ideal values, ranges and satisfactory simulation values have been determined for each of the statistical coefficients (Table 8).

3. Results and discussion

Results are first reported for crop yields, and related biomass and nitrogen stress days, because of the impact that crop production has on the

Table 5
Default HAWQS annual average (2001–2018) elemental nitrogen application rates for corn land use.

Kg/ha of elemental nitrogen applied	% of area		
	DMRB	SSRB	NSRB
64–79	15.0	7.1	20.9
80–99	27.1	39.2	37.0
100–159	13.5	2.6	11.4
160–176	44.4	51.1	30.8

Table 6
Annual elemental nitrogen application rates on corn land use after the management operation update.

Time of the year	Crop rotation	Application rate (Kg/ha)
Fall	Corn-soybean	183
Spring	Corn-soybean	172
Spring	Continuous corn	196

Table 7
Description of model components for the ten baseline simulations with graphical representation of the process logic.

Baseline	Description
[1]	No changes are made, simulation performed with default HAWQS model values
[2]	Same as baseline [1] plus the alternative RCN method (with CNCOEF)
[3]	Same as baseline [1] with improved tile drain map
[4]	Same as baseline [3] with alternative RCN method (with CNCOEF)
[5]	Same as baseline [3] with updated fertilizer application rates
[6]	Same as baseline [5] with alternative RCN method (with CNCOEF)
[7]	Parameters reset to a non-calibrated model with improved tile drain map
[8]	Same as baseline [7] with alternative RCN method (with CNCOEF)
[9]	Same as baseline [7] with updated fertilizer application rates
[10]	Same as baseline [9] with alternative RCN method (with CNCOEF)

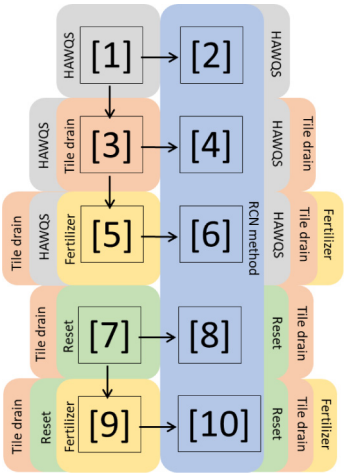

hydrology of the three basins. Water balance and streamflow results are then reported in different graphical and statistical formats to present a comprehensive assessment of the hydrologic impacts of the ten different baseline simulations.

3.1. Crop yield results

The SWAT plant growth component is highly interactive with the hydrological cycle, and crop growth and yield are negatively affected in response to inadequate nitrate fertilizer amounts. The biomass generated by the crop growth model component influences simulated evapotranspiration, soil water content, nutrient uptake, surface runoff and subsurface hydrologic flows that are relevant to hydrological and water quality processes (Arnold et al., 2015). According to Daggupati et al. (2015) and Nair et al. (2011), unsatisfactory streamflow prediction could be caused by a lack of reliable crop growth simulation. They further emphasize that the relationships of biomass and yields in agricultural watersheds are as important as rainfall-runoff processes for water balance estimation. Thus, an assessment of the plant biomass and annual nutrient budgets should be performed to ensure a proper model configuration.

SWAT estimates yields on a dry-weight basis. Therefore, grain yields values were updated on a wet-weight basis of 15.5% moisture for comparison with the U.S. Department of Agriculture (USDA) survey yields (<https://www.nass.usda.gov/AgCensus/index.php>). SWAT was used to predict annual average corn biomass and yields (Table 9) based on the HAWQS default nitrogen application rates (Table 5) and the updated nitrogen application rates (Table 6). The predicted crop yields are compared to the crop yield average for 2016–2020 (Table 9) reported by the USDA in survey data collected for counties located in the study region. Simulated nitrate stress days are also reported (Table 9). Corn yields predicted with the updated N application rates result in values closer to USDA survey-based yields for the DMRB, with a 0.1 t/ha difference for grain yields. The prediction for the SSRB had the same absolute difference (0.6 t/ha) between the non-updated and updated models; however, the non-updated models underestimate and the updated models overestimate the grain yield amounts (Table 9). For the NSRB, both fertilizer application distributions underestimate the total grain yields with the non-updated models resulting in values closer to the survey yields. The updated nitrogen application rates resulted in fewer nitrate stress days for all three basins, versus the nitrate stress days computed using the HAWQS default application rates (Table 9). The highest number of nitrogen stress days was estimated to be

Table 9
Annual average biomass, grain yield (15.5% moisture*), and nitrate stress days for corn crop land use as a function of the HAWQS default nitrogen application rates (Table 5) and updated nitrogen application rates (Table 6).

Basin	Annual average	HAWQS default	Updated	USDA survey
Des Moines River	Biomass (t/ha)	22.9	26.5	x
	Grain yield (t/ha)	10.8	12.5	12.6
	N stress days	20.9	16.8	x
South Skunk River	Biomass (t/ha)	26.0	28.1	x
	Grain yield (t/ha)	12.2	13.4	12.8
	N stress days	16.2	11.6	x
North Skunk River	Biomass (t/ha)	25.4	24.6	x
	Grain yield (t/ha)	12.1	11.7	13.5
	N stress days	15.8	11.42	x

* The SWAT yields were first converted to bu./ac (15.5%) and then both the SWAT and NASS yields were converted back to t/ha. The conversion equation is given by: 15.5%GrainYield (bu/ac) = SimulatedGrainYield(t/ha) * 0.4461 * 2000 * 1.155/56. See Ag Decision Maker (2022) for Metric Conversions.

Table 8
Ideal value, range, and satisfactory simulation of the selected statistical coefficients used for evaluating the performance of the SWAT baselines.

Statistical coefficient	Ideal value	Range	Satisfactory simulation	Reference
Coefficient of determination (R^2)	1	0 to 1	≥0.60	Moriasi et al. (2015)
Nash-Sutcliffe (NS)	1	−∞ to 1	≥0.50	Moriasi et al. (2007 and 2015)
Percent Bias (Pbias)	0	−100% to 100%	±25%	Moriasi et al. (2007 and 2015)
King-Gupta Efficiency (KGE)	1	−∞ to 1	≥0.60	Patil and Stieglitz (2015)

20.9 for the HAWQS default application rates when used for the SWAT DMRB simulations. The nitrogen stress day results further indicate that some of the HAWQS default nitrogen application rates were too low relative to current agronomic requirements for corn.

3.2. Water balance and streamflow results

Overall annual water balance calculations initially determined for the ten baseline simulations included estimates of surface runoff, lateral subsurface flow, tile flow, groundwater (shallow aquifer) flow, water yield and ET (Appendix B). Average annual streamflows were also estimated at the basin outlets (Appendix C). Water balance results were generated as a function of precipitation that varied across the study area from 873 mm/year for the DMRB to 941 and 950 mm/year for the SSRB and NSRB, respectively. Corresponding annual average ET levels varied from 672 to 523 mm/year across the three watersheds. Water balance results reflect the influence of tile drains (Tables B.1 to B.3), with considerably higher tile flows predicted for the DMRB relative to the SSRB and NSRB.

The basin "outlet monitoring gauges" were chosen as those gauges closest to the basin outlets with the most available data, meaning: 05487500 (Runnells) with 9 years of data, 05471500 (Oskaloosa), and 05472500 (Sigourney) with 18 years of data each for the DMRB, SSRB, and NSRB, respectively. Predicted SSRB and NSRB average annual baseline streamflows were similar in magnitude to corresponding observed streamflows. However, predicted DMRB average annual baseline streamflows were below observed streamflows by 52.2 to 98.4 m^3/s except for baseline 3 (Table C.1). Observed streamflow levels were accurately replicated by SWAT for the majority of baseline and gauge combinations (Supplementary material). However, less accurate upstream streamflow predictions for the outlets of the Raccoon River and Middle Des Moines Rivers (gauges 05484900 and 05482000; Supplementary material), coupled with inaccuracies in streamflow predictions in the southern part of the basin, led to large underpredictions near the DRMB outlet. These results underscore the need for calibration in the next phase of research.

The WHAT filter resulted in annual average baseflow values of 229.7 mm, 214.4 mm, and 158.9 mm for the DMRB, SSRB and NSRB, respectively. Corresponding annual average surface runoff levels calculated by the WHAT filter were 81.6 mm, 101.3 mm, and 105.3 mm for the DMRB, SSRB and NSRB. Observed baseflow proportions of overall flow, based on the WHAT calculations, were 72.8%, 67.9% and 60.1% for the DMRB, SSRB and NSRB (Fig. 5). Similar values were also reported by Schilling et al. (2021) for the same region. The dominant effect of baseflow on the hydrographs can be expected in heavily tile drained areas (Schilling et al., 2019, 2021).

Simulated baseflow and surface runoff values were compared for the ten different baselines (Fig. 5). The left axis shows total annual averages in mm and the right axis presents the percentages compared to streamflow. Simulated baseflows represent the composite lateral flow, tile drainage, and groundwater recharge (shallow aquifer) flows estimated by SWAT. Predicted baseflow and surface runoff water balance outputs were compared to observed data (WHAT filter) for the ten baseline cases.

Different model inputs (Table 7) led to marked variation in annual water balance averages estimated for these watersheds (Fig. 5). Generally, use of the CNCOEF in the alternative RCN method resulted in higher estimates of baseflow for the five baseline simulations in which it was applied (2, 4, 6, 8 and 10) for all three basins. The simulated baseflow values for the DMRB ranged from 43.2 mm/year (baseline 9) to 203.5 mm/year (baseline 2). Baseline 2 resulted in value closest to observed DMRB baseflow; however, this represents 95.8% of total streamflow for the current simulation, which is an unrealistic fraction for the region (Schilling et al., 2021). The DMRB baseline 8 produced a value closest to the observed data for annual surface runoff (70.2 mm/year), and also resulted in reasonable ratios of 73.1% for baseflow and 26.9% for surface runoff. The North and South Skunk basins present the same changing behavior between the baselines, where (1) the predicted annual contribution of surface runoff ranged from 65.1 mm (SSRB baseline 10) to 217.3 mm (NSRB baseline 3), and (2) the baseflow varied from 102.6 mm (SSRB baseline 7) to 283.6 mm (NSRB baseline 4). The SSRB baseline 8 resulted in the smallest difference

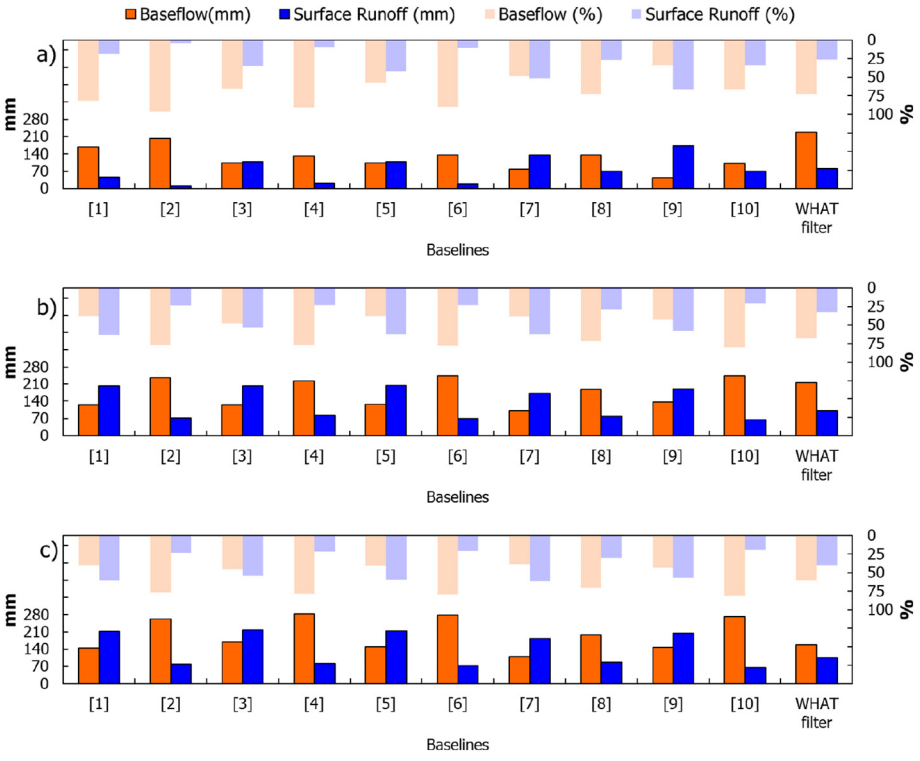

Fig. 5. Simulated annual average baseflow and surface runoff, for (a) Des Moines River Basin, (b) South Skunk River Basin, and (c) North Skunk River Basin, where the left axis show total annual averages in mm and the right axis indicates the percentage compared to water yield.

(in mm) between observed and simulated baseflow and surface runoff. The resulting baseflow and surface runoff percentages were 71.2% and 28.8% for streamflow, respectively, which is consistent with observed WHAT proportions of 67.9% and 32.1% for SSRB baseflow and surface runoff. The NSRB baseline 5 provides the best estimate of baseflow magnitude (158.8 mm); however, the proportions of 40.7% for baseflow and 59.3% for surface runoff are not realistic for intensively tile drained areas. The NSRB baseline 8 again resulted in the best estimates for surface runoff (87.9 mm) and baseflow (197.7 mm) and in more realistic proportions of 70.3% for baseflow and 29.7% for surface runoff of total streamflow.

3.3. Spatial representation of streamflows

Spatial comparisons were created for all ten baselines (Table 7) between observed and simulated streamflows for the subbasins draining to the different gauge locations (Fig. 6). Statistical results of the spatial representations are shown in two ways: (1) six levels of shading for the NS statistics that range from red to green, where red denotes the weakest simulation results, and (2) Pbias levels, which are represented by light blue triangles if the model underpredicted the measured streamflows or dark blue triangles if the model overpredicted the corresponding streamflows. Besides providing analyses of subbasin outlets, the results for all streamflow stations provide valuable spatial information about model dynamics for the different baselines. For example, the simulations for baselines 3 and 6 would be equally poor (NS < 0) if only the DMRB outlet were analyzed, which is not accurate if results for upstream monitoring gauges are considered.

This spatially explicit assessment also reveals simulation problems at the subbasin level. For example, the subbasin in the northern part of the SSRB (that drains to USGS gauge 05470000; Supplementary material) is red in all ten baselines (Fig. 6), reflecting weak simulation results. Accurate streamflows were difficult to achieve for this gauge, resulting in baseline model simulations consistently overpredicting streamflow (Pbias dark blue triangles). This is likely due to subsurface geology in the floodplain of the basin where recent alluvium overlies an unusually thick (20–30 m) deposit of medium to pebbly sand outwash (Quade et al., 2001). Groundwater monitoring in the Skunk River floodplain has indicated that surface water infiltrates into the alluvium as a losing stream in this area, contributing herbicides to the alluvial aquifer (Burkart et al., 1999). Model simulations do not account for loss of surface water into the alluvial aquifer as river discharge infiltrates into the layers of thick outwash. Hence, streamflows were consistently overpredicted for this portion of the Skunk River due to this stream segment effectively functioning as a continuous "losing stream". Future calibration and validation phases will incorporate methods to address this characteristic of the Skunk River segment, including possible adaptation of karst geology modeling methods (e.g., see Eini et al. (2020)).

The default HAWQS model was not improved by the addition of the improved tile drain map (Fig. 4 and Table 4), as evidenced by baseline 3 and 4 producing the most poorly simulated subbasins (Fig. 6). However, the incorporation of improved nitrogen fertilizer application rates in baselines 5 and 6 considerably improved results (NS > 0.49) as shown by the corresponding maps (Fig. 6). In contrast, implementation of the improved tile drain map for the four "reset baselines" (baselines 7–10, Table 7) produced consistent improvement in general model performance (Fig. 6). Baselines 5 and 7 produced the best performance for the DMRB, and both SSRB and NSRB respectively, based on median NS values. In general, overall model performance was stronger for the DMRB relative to the combined SSRB and NSRB.

Considering the NS criterion of 0.50 (Table 8) the SWAT modeling results were always satisfactory regardless of baseline (Table 7) for 10 gauge stations (Fig. 1). However, unsatisfactory NS results (NS < 0.50) were always found for 9 of the other stations. Based on averages, the NS varied from 0.60 (baselines 5 and 10) to −0.16 (baseline 3) for the DMRB, 0.78 (baseline 7) to 0.42 (baseline 4) for the NSRB, and −0.23 (baseline 4) to 0.54 (baseline 7) for the SSRB. It is important to mention that two outlier stations that manifested NS values consistently below zero (USGS gauges 05470000 and 05487540; Supplementary Material) were removed from the average calculations. In analysis of the three basin outlets, the NS values ranged from 0.52 (baseline 8) to 0.80 (baseline 9) for the DMRB; 0.33 (baseline 4) to 0.80 (baseline 9) for the SSRB, and 0.42 (baseline 4) to 0.78 (baseline 7) for the NSRB. Acceptable Pbias results

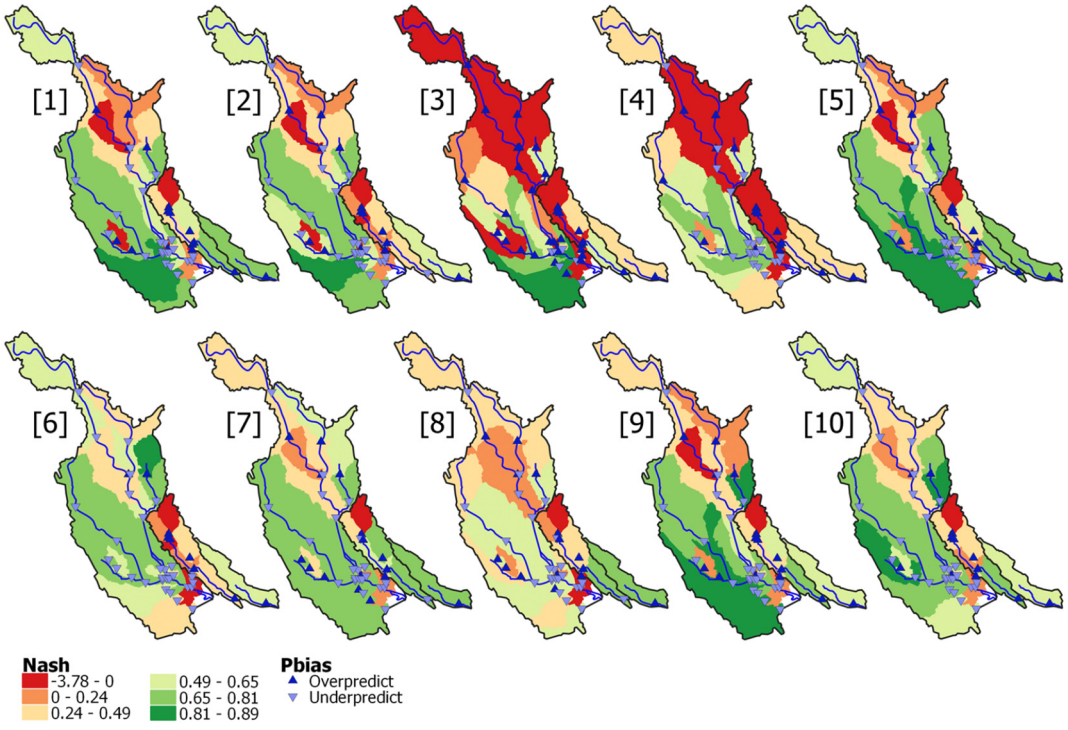

Fig. 6. Spatial representation of Nash-Sutcliffe and Pbias values for the simulated DMBR, SSBR and NSBR subbasins.

(±25%; Table 8) were reported for almost all predicted streamflow and gauge combinations, except for USGS gauge 05470000 in the northern part of the SSRB (shown in red for NS values for all ten baselines; Fig. 6). For the three basin outlets Pbias ranged from: (1) +46.4% (baseline 6) to +1.6% (baseline 3) for the DMRB, (2) −23.8% (baseline 3) and +11.5% (baseline 8) to for the SSRB, and (3) −54% (baseline 3) to −13% (baseline 8) for the NSRB.

R^2 statistics were generated for all 40 monitoring stations (Supplementary material). Computed R^2 averages ranged from: 0.79 (baseline 5) to 0.54 (baseline 8) for the DMRB, 0.76 (baseline 9) to 0.24 (baseline 4) for the SSRB, and 0.81 (baselines 1 and 7) to 0.64 (baseline 4) for the NSRB. Considering all monitoring gauges, baselines 5 and 7 produced the best results with an R^2 average of 0.77; baseline 8 performed at an unsatisfactory average (R^2 = 0.55) considering the criterion of 0.60 (Table 8). Most R^2 values were above this criterion level and in the absence of any specific calibration the baselines and observed data indicated a good correlation.

3.4. Further analysis of outlet streamflows

Scatter plot and histogram comparisons were developed between observed and simulated SWAT streamflow data for all ten baselines, for the gauge sites nearest the DMRB (years compared: 2001 to 2009), SSRB (years compared: 2001 to 2018) and NSRB (years compared: 2001 to 2018) outlets (Fig. 5). Average annual streamflow levels were also determined for the three outlets (Appendix C, Table C.1). Correlation graphs together with R^2 values and histograms for all 40 monitoring streamflow stations were also analyzed (Supplementary material).

R^2 values were satisfactory (R^2 > 0.60; Table 8) for all of the DMRB baselines except baseline 6, indicating that the majority of baselines could replicate the streamflow trends. Baseline 9 (R^2 = 0.80) resulted in the best agreement on the basis of both the R^2 and histogram (Fig. 7), indicating a robust linear relationship between observed and simulated data. The SSRB streamflow was most accurately reproduced by baselines 9, 5, 7, 1, 10 and 6; however, predicted streamflows for baselines 2, 3, 4, and 8 resulted

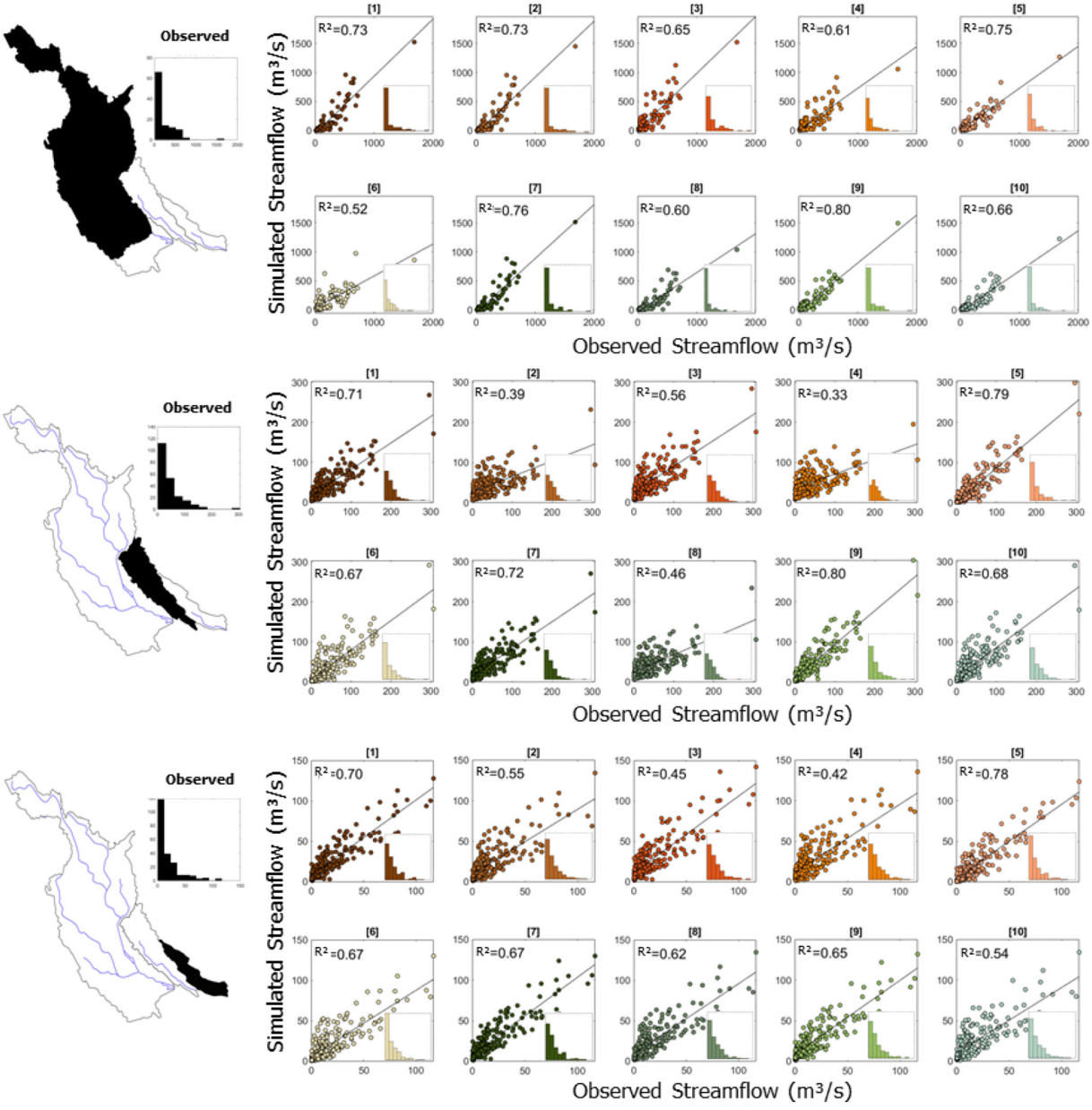

Fig. 7. Observed versus simulated streamflow for each baseline applied to the three basins.

in weaker R^2 values that were <0.60. The highest SSRB R^2 was found for baseline 9 (0.80) which also manifested a histogram that accurately reflected observed streamflow characteristics. For the NSRB, baseline 5 resulted in the best R^2 (0.78) and histogram simulation results followed by baselines 1, 7, 6, 9 and 8, which all produced R^2 values >0.60. In contrast, predicted streamflows for baselines 2, 3, 4, and 10 all resulted in R^2 values <0.60. Respective top performances of baseline 9 (DMRB and SSRB) and baseline 5 (NSRB) underscore the more accurate hydrologic replication that resulted from implementation of the improved tile drain map (Fig. 4 and Table 4), and improved crop yield (and implicitly crop biomass) estimation due to the updated nitrogen fertilizer applications (Table 6).

Flow Duration Curves (FDCs; Fig. 8) were calculated using the entire time series for the same gauges shown in Fig. 7. Our analysis of these is based on visual similarity between observed and simulated streamflow, and the nonparametric Two-Sample Kolmogorov-Smirnov test (two-sample K-S test) statistic (Feller, 1948). The FDCs can also be used to analyze reproduction of streamflow volume. The baseline simulations performed best during very high flow conditions (95%) for all three basins. The mid streamflow segment (50%) was underestimated by all of the baselines for the DMRB and overestimated for all of the simulated NSRB baselines. For the SSRB, the mean streamflow was underestimated by baselines 7 and 8, and overestimated by the other baselines. The 20% of lowest flows were underestimated for all baselines for the DMRB, and by SSRB baselines 7 and 8. The NSRB streamflow was overestimated by all baselines for the lowest 20% segment; baselines 7 and 8 resulted in the best curve fit. Flow duration curves graphs were also produced for all 40 monitoring streamflow stations (Supplementary material).

The two-sample K-S test evaluates the difference between the probability distributions of two samples; smaller test values indicate more similarity between flow duration curves. The test was applied to the entire time series, and the DMRB baseline 7 produced the closest curve to the observed data, followed by DMRB baselines 8 and 9. For the SSRB, baseline 8 has better K-S test representation followed by baselines 10 and 7, and the NSRB FDC was also better expressed by baseline 8, followed by baselines 7 and 2 (Appendix D).

3.5. Evaluation of seasonal simulation results

In addition to total time series analyses, it is essential to investigate specific time periods within the SWAT simulations, including snowmelt (February, through April) and the growing season (May through September). The entire time series, and snowmelt and growing season time periods, were evaluated as a function of all four statistical coefficients (NS, R^2, KGE and Pbias, Section 2.8) (Fig. 9). Baseline simulations with the strongest results (blue coloration) were compared to the weakest (red coloration) for all streamflow monitoring stations, to rank the baselines. For example, baseline 7 produced the strongest NS results for SSRB for 5 out of 7 stations.

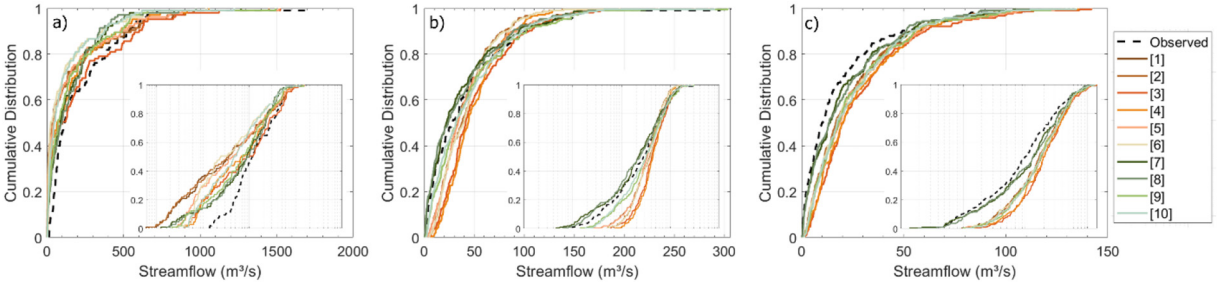

Fig. 8. Flow duration curves for the ten baseline simulations and observed data for a) Des Moines River Basin, b) South Skunk River Basin and c) North Skunk River Basin (the log format of the FDC is shown at the bottom right corner of the graphs).

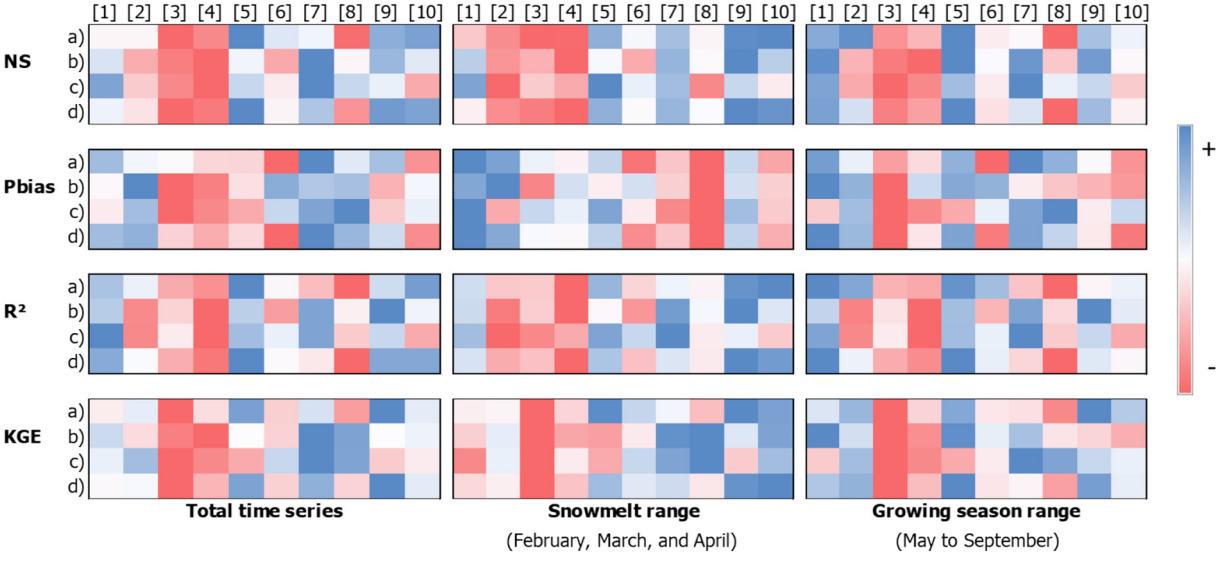

Fig. 9. Baseline rankings for the monitoring gauges. a) Des Moines River basin (32 stations), b) South Skunk River basin (7 stations), c) North Skunk River basin (1 station), d) sum of all three systems (40 stations). Baselines that produced better simulations are indicated in blue.

When we evaluate the four statistical coefficients together (NS, R^2, KGE, and Pbias), the three basins (DMRB, SSRB, and NSRB), and all the time series division (total, snowmelt, and growing season), the SWAT simulations that generate the best overall results are for baselines 9 and 5. The snowmelt season showed similar ranking behavior for NS, R^2 and KGE, with baselines 9 and 10 performing better. However, better Pbias results occurred for baselines 1 and 2 (Fig. 9(d)). Rankings computed for the four statistical criteria are similar for the growing season, although only baselines 1 and 5 resulted in consistently high trends (Fig. 9(d)).

For the DMRB total time series (Fig. 9), baseline 5 produced the highest rankings for NS and R^2; baseline 9 ranked first for KGE, and baseline 7 had the strongest Pbias results. However, for the DMRB snowmelt period, baselines 10 and 9 exhibited the strongest NS, R^2 and KGE statistics, and Baseline 1 the most accurate Pbias values. Individual baselines produced best results for each of the four statistics during the growing season for DMRB: baselines 5, 7, 1 and 9 for NS, Pbias, R^2 and KGE, respectively. Regarding the SSRB total time series (Fig. 9), baselines 7 and 9 resulted in the strongest respective NS, KGE, and R^2 statistics; the Pbias was more accurate for baseline 1. The SSRB snowmelt season was ranked as: baseline 9 for the NS and R^2, baseline 2 for the Pbias, and baseline 8 for the KGE. The SSRB growing season is better represented by baselines 1 and 5; however, baseline 9 produced the strongest R^2 value. For the NSRB total time series and considering the four statistics, the baselines 7, 8, and 1 were most highly ranked; the snowmelt season resulted in one highly ranked baseline per each statistical coefficient: baselines 5, 1, 7, and 8, respectively, for the NS, Pbias, R^2, and KGE. The growing season was better ranked by the baseline 7 for the NS, R^2, and KGE; regarding the NSRB Pbias, baseline 8 resulted in the strongest simulation. In general, baselines 3 and 4 resulted in the most inaccurate SWAT simulations on the basis of the four statistics across the different time periods and the three basins (Fig. 9).

3.6. Discussion

The tests of the 10 baselines (Table 7) present an intriguing and in some ways conflicting set of results. Analyses of the suite of four statistics (Fig. 9) revealed that SWAT baselines 1, 5, 7 and 9 generated the most consistently accurate streamflows on the basis of those statistical evaluations. However, the same four baselines also resulted in inaccurate partitioning of baseflow versus surface runoff (Fig. 5) with the exception of the DMRB baseline 1 simulation. As noted previously, baseline 8 produced the most accurate partitioning between baseflow and surface runoff but was characterized by relatively weak statistics, especially for the DMRB (Fig. 9). The weak statistical performance for baseline 8 may be due in part to underprediction of total streamflow at the gauge used to assess "outlet streamflow" as previously discussed. Similar dichotomies in the results can be discerned for the streamflow partitioning results (Fig. 5) versus aggregated statistical evaluation (Fig. 9).

The particularly weak statistical results for baselines 3 and 4 (Fig. 5) are reinforced by spatial statistical analyses (Fig. 6). The spatial maps also reveal that the baseline 8 simulation was relatively weak compared with the majority of other simulated baselines. Stronger spatial statistical results were found when the improved nitrogen fertilizer application rates were incorporated in baselines 9 and 10, which generally resulted in more accurate crop yields, probable improved biomass estimates and in turn more accurate hydrologic results. Notably, baseline 9 also resulted in the strongest R^2 and hydrologic histogram results for the DMRB and SSRB (Fig. 7). However, the NSRB was best represented by baseline 5 in terms of the strongest R^2 and replication of the observed hydrologic histogram (Fig. 7). In general, the NSRB baseline simulations were the least affected by incorporation of the improved tile drain map and/or fertilizer applications.

Overall, these results clearly point to the need to consider the most accurate input data available and logical hydrologic results, in combination with graphical and statistical analyses, to determine the most accurate replication of the hydrological characteristics of a basin simulated in SWAT. The application of the alternative RCN method, calculated on the basis of ET and the curve number coefficient (CNCOEF), was the only way that the dominant baseflow fraction was accounted for (Fig. 5; baselines 2, 4, 6, 8 and 10). However, weak statistical results were only overcome with incorporation of both the improved tile drain map and nitrogen fertilizer application rates (e.g., baseline 10). These results also underscore the need for comprehensive calibration and validation of the DMRB, SSRB and NSRB, taking into account 'real system data' and other factors discussed here. Baseline 5 (Table 7) represents a partial step in that direction based on the initial HAWQS calibration and improved input data. Overall, the baseline analyses performed in this study provide a strong foundation to conduct the next phase of calibration and validation for the DMRB, SSRB and NSRB.

4. Conclusion

The continuous and physically-based ecohydrological model, SWAT, was used to investigate hydrologic representations for the Des Moines River Basin (DMRB), South Skunk River Basin (SSRB), and North Skunk River Basin (NSRB) using a variety of 'real system data'. Ten baseline simulations were built starting with a default SWAT model offered by the HAWQS platform (baseline 1) and replacing input data (Table 7) to address the following goals: (1) identifying the importance of accurate representation of tile drain locations, density and model input parameters, (2) quantifying the effects of different amounts of N fertilizer applications on corn biomass production and grain yields, (3) analyzing the impacts of different surface runoff methods on water balance calculation, (4) identifying accurate baseflow performance, and (5) evaluating the spatial efficiency of SWAT model simulations based on statistical and graphical measures. Baseline responses were analyzed using simulated streamflows and compared with observed records at 40 monitoring gauges. The main outcomes were:

- Baseflow estimation was higher for the five baselines in which the alternative RCN method (CNCOEF) was applied. Baseline 8 (Fig. 5 and Table 7) produced the closest surface runoff and baseflow values compared to annual observed data, as a function of the alternative RCN method and tile drain map.
- Baselines with N fertilizer application updates presented values closer to the USDA Census Survey (corn yields) for the DMRB, and fewer nitrate stress days for all three basins.
- According to median NS values, baseline 9 (Fig. 6 and Table 7) resulted in the best performance for DMRB and baseline 7 (Fig. 6 and Table 7) for the SSRB and NSRB. Baseline 9 produced the most consistent set of strong statistical results (NS, KGE, R^2 and Pbias), followed by baselines 5, 7 and 1, respectively.
- The spatial variability of monitoring gauges across the study area improved SWAT model performance, and helped identify simulation problems at the subbasin level.
- The top performances of baseline simulations 5, 7, 8, and 9 underscore that more accurate hydrological replication resulted due to the improved tile drain map and enhanced crop yield estimation (using updated nitrogen fertilizer application inputs).
- The HAWQS platform proved to be useful in generating SWAT models from a time and computational memory perspective, since all projects can be managed/modified online. However, several improvements are suggested for the platform, such as incorporating a more refined soil map (e.g., Soil Survey Geographic Database - SSURGO), implementing a detailed tile drain map for model default simulations based on the approach described in this study (Fig. 4 and Table 4), and reviewing management operations including revised nitrogen fertilizers applications for specific crops; e.g., corn production (The HAWQS input data documentation (Texas A&M, 2017) cites White et al. (2016) as the source of the management data; revisions to these data are likely needed).

Overall, this study indicates the importance of carefully selected input data that accurately represents the hydrological processes of a simulated watershed. The results also underscore the benefits of model testing using multiple stream monitoring gauges, if such data are available. Additionally,

use of multiple statistical criteria and multi-site applications are required to accurately represent and identify the ecohydrological behavior in a target study area. The relevance of 'real system data' was reaffirmed by the fact that we can obtain good statistical results based on default data. However, that ignores problems in the model structure that can lead to greater problems in subsequent scenario applications (especially errors in simulated pollutant transport). For example, the North Skunk River basin baseline 1 presented satisfactory statistics (NS = 0.70); however, it has a relationship between surface runoff (60%) and baseflow (40%) that does not represent the reality expected in heavily tile drained areas (dominant baseflow). Further work will focus on additional testing of specific baselines (5, 7, 8, 9), including essential characteristics identified in this research: tile drain map, updated N applications, and alternative RCN method. Additional steps are needed to improve the SWAT baseline configuration including the implementation of the more refined Soil Survey Geographic Database (SSURGO) data (USDA-NRCS, 2022a, 2022b, 2022c), review and possible revisions of various management operations, comparison of the model's performance for different output data (i.e. suspended sediments, nitrate load, and phosphorus load), automatic calibration strategy, and accounting for sources of uncertainty (i.e. model configuration, observed data, epistemic errors) involved in model evaluation.

CRediT authorship contribution statement

Tássia Mattos Brighenti: Conceptualization, Methodology, Software, Validation, Formal analysis, Investigation, Resources, Writing - Original Draft, Writing - Review & Editing, Visualization, Supervision, Project administration.

Philip W. Gassman: Conceptualization, Methodology, Validation, Formal analysis, Investigation, Writing - Original Draft, Writing - Review & Editing, Supervision, Project administration, Funding acquisition.

Keith E. Schilling: Conceptualization, Formal analysis, Investigation, Writing - Review & Editing.

Raghavan Srinivasan: Formal analysis, Investigation, Writing - Review & Editing.

Matt Liebman: Conceptualization, Formal analysis, Investigation, Writing - Review & Editing, Funding acquisition.

Jan R. Thompson: Conceptualization, Formal analysis, Investigation, Writing - Review & Editing, Funding acquisition.

Declaration of competing interest

The authors declare that they have no known competing financial interests or personal relationships that could have appeared to influence the work reported in this paper.

Acknowledgments

The authors acknowledge the National Science Foundation (NSF) Award # 1855902 – for financial support of this work.

Appendix A

Table A.1
SWAT parameters for HAWQS configuration and for the reset SWAT model.

Definition of adjusted SWAT parameter	SWAT parameter name	HAWQS DMRB	HAWQS SSRB	HAWQS NSRB	Reset
Curve number calculation method (0 versus 1)	ICN	0	0	0	0/1
Plant ET curve number coefficient	CNCOEF	x	x	x	x/0.75
Soil evaporation compensation factor	ESCO	0.801	0.95	0.95	0.95
Depth to subsurface drain (mm)	DDRAIN	1420	1200	1200	1200
Depth to impervious layer in soil profile (mm)	DEP_IMP	1827	4000	0	6000
Time to drain soil to field capacity (hours)	TDRAIN	72	72	72	24
Drain tile lag time (hours)	GDRAIN	48	48	48	48
Surface runoff lag	SURLAG	4	2	4	4
Delay time for aquifer recharge (days)	GW_DELAY	73.95	102	30	31
Baseflow recession constant	ALPHA_BF	0.6717	0.023	0.077	0.048
Threshold water level in shallow aquifer for base flow (mm)	GWQMN	3912	900	900	1000
Revap coefficient	GW_REVAP	0.1197	0.02	0.02	0.02
Threshold water level in shallow aquifer for revap (mm)	REVAPMN	377.5	500	500	750
Aquifer percolation coefficient	RCHRG_DP	0.0525	0.05	0.05	0.05

Appendix B

Table B.1
Water balance values (mm).

Des Moines River basin (DMRB)						
Baseline	Surface runoff	Lateral flow	Tile	Groundwater (shal aq)	Water yield	ET
[1]	47.49	4.91	164.19	0	216.57	651.1
[2]	10.76	5.63	197.83	0	214.65	651.7
[3]	132.50	19.32	113.60	0	264.62	604.9
[4]	21.58	31.85	147.36	0	200.58	630.8
[5]	107.87	16.90	86.12	0	210.26	656.4
[6]	19.37	29.15	107.99	0	156.32	672.1
[7]	136.28	2.68	0.21	74.75	217.76	629.6
[8]	70.15	3.27	1.17	132.75	214.54	632.4
[9]	173.92	12.21	30.94	0.04	216.03	650.8
[10]	69.27	25.68	74.94	0.15	169.47	673.1

Table B.2
Water balance values (mm).

South Skunk River basin (SSRB)						
Baseline	Surface runoff	Lateral flow	Tile	Groundwater (shal aq)	Water yield	ET
[1]	202.02	1.94	0.03	123.78	325.21	582.8
[2]	72.09	2.65	0.16	236.14	309.91	589.2
[3]	235.46	1.91	2.23	147.31	384.07	524.7
[4]	48.12	2.93	15.58	297.30	363.06	533.7
[5]	202.53	1.95	1.86	124.20	327.98	580.3
[6]	70.16	2.67	10.28	231.56	313.57	586.1
[7]	170.89	2.12	1.91	98.59	278.37	634.5
[8]	78.88	2.69	8.12	177.02	276.09	637.1
[9]	189.88	2.24	2.25	131.84	332.62	583.7
[10]	65.13	2.96	10.57	232.03	322.96	593.1

Table B.3
Water balance values (mm).

North Skunk River basin (NSRB)						
Baseline	Surface runoff	Lateral flow	Tile	Groundwater (shal aq)	Water yield	ET
[1]	210.53	0.60	0	142.66	351.45	571.6
[2]	78.52	0.84	0.01	260.55	338.82	577.5
[3]	238.51	0.71	5.22	158.04	400.01	523.7
[4]	51.77	1.10	35.18	296.82	383.96	531.4
[5]	213.93	0.72	4.71	142.96	360.01	563.7
[6]	71.75	1.02	24.52	252.31	348.55	568.6
[7]	183.52	0.68	5.05	103.48	297.01	628.8
[8]	87.27	0.89	19.30	177.65	294.07	631.8
[9]	203.48	0.73	5.69	139.08	354.90	573.3
[10]	66.80	1.01	26.03	243.67	350.09	577.1

Appendix C

Table C.1
Observed and simulated streamflows at the basin outlets.

Baseline	Streamflow (m^3/s)		
	DMRB[a]	SSRB[a]	NSRB[a]
Observed	212.2	42.6	18.6
[1]	157.9	44.4	25.2
[2]	156.3	42.2	24.3
[3]	208.7	52.7	28.7
[4]	159.9	49.8	27.5
[5]	151.2	44.7	25.9
[6]	113.8	42.7	25.0
[7]	154.2	38.0	21.3
[8]	150.8	37.7	21.1
[9]	154.9	45.3	25.5
[10]	120.8	43.9	25.1

[a] Outlet USGS gauges: 05487500 (Runnells) (DMRB) – drainage area: 30186.3 km^2; 05471500 (Oskaloosa) (SSRB) - drainage area: 4234.6 km^2; and 05472500 (Sigourney) (NSRB) - drainage area: 1890.7 km^2.

Appendix D

Table D.1
Two-sample Kolmogorov-Smirnov test values at the basin outlets.

	DMRB[a]	SSRB[a]	NSRB[a]
[1]	0.4000	0.2037	0.2222
[2]	0.4000	0.2361	0.2037
[3]	0.2762	0.2824	0.2963
[4]	0.3238	0.3056	0.287
[5]	0.3714	0.2037	0.2269
[6]	0.4190	0.2454	0.2176
[7]	0.2000	0.0880	0.1343
[8]	0.2190	0.0787	0.1157
[9]	0.2381	0.1157	0.2222
[10]	0.3238	0.0833	0.2222

[a] Outlet USGS gauges: 05487500 (Runnells) (DMRB); 05471500 (Oskaloosa) (SSRB); and 05472500 (Sigourney) (NSRB).

Appendix E. Supplementary data

Supplementary data to this article can be found online at https://doi.org/10.1016/j.scitotenv.2022.156302.

References

Abbaspour, K.C., Rouholahnejad, E., Vaghefi, S., Srinivasan, R., Yang, H., Kløve, B., 2015. A continental-scale hydrology and water quality model for europe: calibration and uncertainty of a high-resolution large-scale SWAT model. J. Hydrol. 524, 733–752. https://doi.org/10.1016/j.jhydrol.2015.03.027.

Acero Triana, J.S., Chu, M.L., Guzman, J.A., Moriasi, D.N., Steiner, J.L., 2019. Beyond model metrics: the perils of calibrating hydrologic models. J. Hydrol. 578, 124032. https://doi.org/10.1016/j.jhydrol.2019.124032.

Ackerman, K., Conard, M., Culligan, P., Plunz, R., Sutto, M.P., Whittinghill, L., 2014. Sustainable food systems for future cities: the potential of urban agriculture. Econ. Soc. Rev. (Irel). 45, 189–206.

Ag Decision Maker, 2022. Available online: https://www.extension.iastate.edu/agdm/wholefarm/pdf/c6-80.pdf.

Akoko, G., Le, T.H., Gomi, T., Kato, T., 2021. A review of swat model application in africa. Water (Switzerland) 13. https://doi.org/10.3390/w13091313.

Andréassian, V., Le Moine, N., Perrin, C., Ramos, M.H., Oudin, L., Mathevet, T., Lerat, J., Berthet, L., 2012. All that glitters is not gold: the case of calibrating hydrological models. Hydrol. Process. 26, 2206–2210. https://doi.org/10.1002/hyp.9264.

Arnold, J.G., Srinivasan, R., Muttiah, R.S., Williams, J.R., 1998. Large area hydrologic modeling and assessment part I: Model development. J. American Water Res. Assoc. 34 (1), 73–89. https://doi.org/10.1111/j.1752-1688.1998.tb05961.x.

Arnold, J.G., Moriasi, D.N., Gassman, P.W., Abbaspour, K.C., White, M.J., Srinivasan, R., Santhi, C., Harmel, R.D., Griensven, a. Van, VanLiew, M.W., Kannan, N., Jha, M.K., 2012. SWAT: model use, calibration, and validation. Trans. ASABE 55, 1491–1508.

Arnold, J.G., Youssef, M.A., Yen, H., White, M.J., Sheshukov, A.Y., Sadeghi, A.M., Moriasi, D.N., Steiner, J.L., Amatya, D.M., Skaggs, R.W., Haney, E.B., Jeong, J., Arabi, M., Gowda, P.H., 2015. Hydrological processes and model representation: impact of soft data on calibration. Trans. ASABE 58, 1637–1660. https://doi.org/10.13031/trans.58.10726.

Béné, C., Oosterveer, P., Lamotte, L., Brouwer, I.D., de Haan, S., Prager, S.D., Talsma, E.F., Khoury, C.K., 2019. When food systems meet sustainability – current narratives and implications for actions. World Dev. 113, 116–130. https://doi.org/10.1016/j.worlddev.2018.08.011.

Beven, K., 2019. How to make advances in hydrological modelling. Hydrol. Res. 50, 1481–1494. https://doi.org/10.2166/nh.2019.134.

Bieger, K., Arnold, J.G., Rathjens, H., White, M.J., Bosch, D.D., Allen, P.M., Volk, M., Srinivasan, R., 2017. Introduction to SWAT+, a completely restructured version of the Soil and Water Assessment Tool. J. Am. Water Resour. Assoc. 53, 115–130. https://doi.org/10.1111/1752-1688.12482.

Brighenti, T.M., Bonumá, N.B., Srinivasan, R., Chaffe, P.L.B, 2019. Simulating sub-daily hydrological process with SWAT: a review. Hydrol. Sci. J., 1415–1423 https://doi.org/10.1080/02626667.2019.1642477.

Burkart, M.R., Simpkins, W.W., Squillace, P.J., Helmke, M., 1999. Tributary stream infiltration as a source of herbicides in an alluvial aquifer. J. Environ. Qual. 28 (1), 69–74.

CARD, 2022. SWAT Literature Database for Peer-Reviewed Journal Articles. Iowa State University, Ames, IA, Center for Agricultural and Rural Development. https://www.card.iastate.edu/swat_articles/.

Chen, M., Gassman, P.W., Srinivasan, R., Cui, Y., Arritt, R., 2020. Analysis of alternative climate datasets and evapotranspiration methods for the Upper Mississippi River Basin using SWAT within HAWQS. Sci. Total Environ. 720, 137562. https://doi.org/10.1016/j.scitotenv.2020.137562.

Chen, M., Cui, Y., Gassman, P.W., Srinivasan, R., 2021. Effect of watershed delineation and climate datasets density on runoff predictions for the Upper Mississippi River Basin using SWAT within HAWQS. Water (Switzerland) 13. https://doi.org/10.3390/w13040422.

Daggupati, N., Pai, S., Ale, K.R., Douglas-Mankin, R.W., Zeckoski, J., Jeong, P.B., Parajuli, D., Saraswat, M.A., Youssef, 2015. A recommended calibration and validation strategy for hydrologic and water quality models. Trans. ASABE 58 (6), 1705–1719. https://doi.org/10.13031/trans.58.10712.

Daggupati, P., Deb, D., Srinivasan, R., Yeganantham, D., Mehta, V.M., Rosenberg, N.J., 2016. Large-Scale Fine-Resolution Hydrological modeling using parameter regionalization in the Missouri River Basin. J. Am. Water Resour. Assoc. 52, 648–666. https://doi.org/10.1111/1752-1688.12413.

Dai, J., Wu, S., Han, G., Weinberg, J., Xie, X., Wu, X., Song, X., Jia, B., Xue, W., Yang, Q., 2018. Water-energy nexus: a review of methods and tools for macro-assessment. Appl. Energy 210, 393–408. https://doi.org/10.1016/j.apenergy.2017.08.243.

Daly, C., Halbleib, M., Smith, J.I., Gibson, W.P., Doggett, M.K., Taylor, G.H., Curtis, J., Pasteris, P.P., 2008. Physiographically sensitive mapping of climatological temperature and precipitation across the conterminous United States. Int. J. Climatol. 28 (15), 2031–2064. https://doi.org/10.1002/joc.1688.

Bressiani, D. de A., Gassman, P.W., Fernandes, J.G., Garbossa, L.H.P., Srinivasan, R., Bonumá, N.B., Mendiondo, E.M., 2015. A review of soil and water assessment tool (SWAT) applications in Brazil: challenges and prospects. Int. J. Agric. Biol. Eng. 8, 1–27. https://doi.org/10.3965/j.ijabe.20150803.1765.

DMMSA; US OMB, 2018. OMB Bulletin No. 18-03. Office of Management and Budget. https://www.whitehouse.gov/wp-content/uploads/2018/04/OMB-BULLETIN-NO.-18-03-Final.pdf.

Eini, M.R., Javadi, S., Delavar, M., Gassman, P.W., Jarihani, B., 2020. Development of alternative SWAT-based models for simulating water budget components and streamflow for a karstic-influenced watershed. Catena. 195, 104801. https://doi.org/10.1016/j.catena.2020.104801.

Feller, W., 1948. On the Kolmogorov-Smirnov limit theorems for empirical distributions. Ann. Math. Stat. 19 (2), 177–189. https://doi.org/10.1214/aoms/1177730243.

Gassman, P.W., Wang, Y., 2015. IJABE SWAT Special Issue: innovative modeling solutions for water resource problems. Int. J. Agric. Biol. Eng. 8. https://doi.org/10.3965/j.ijabe.20150803.1763.

Gassman, P.P.W., Reyes, M.M.R., Green, C.C.H., Arnold, J.J.G., 2007. The Soil and Water Assessment Tool: historical development, applications, and future research directions. Trans. ASAE 50, 1211–1250 10.1.1.88.6554.

Gassman, P.W., Sadeghi, A.M., Srinivasan, R., 2014. Applications of the SWAT model (Special Section): overview and insights. J. Environ. Qual. 43, 1. https://doi.org/10.2134/jeq2013.11.0466.

Gassman, P.W., Valcu-Lisman, A.M., Kling, C.L., Mickelson, S.K., Panagopoulos, Y., Cibin, R., Chaubey, I., Wolter, C.F., Schilling, K.E., 2017a. Assessment of bioenergy cropping scenarios for the Boone River watershed in north central Iowa, United States. J. Am. Water Resour. Assoc. 53, 1336–1354. https://doi.org/10.1111/1752-1688.12593.

Gassman, P.W., Valcu-Lisman, A.M., Kling, C.L., Mickelson, S.K., Panagopoulos, Y., Cibin, R., Chaubey, I., Wolter, C.F., Schilling, K.E., 2017b. Supporting information for "Assessment of bioenergy cropping scenarios for the Boone River watershed in north central Iowa, United States.". J. Am. Water Resour. Assoc. 53, 1336–1354. https://doi.org/10.1111/1752-1688.12593.

Gassman, P.W., Jeong, J., Boulange, J., Narasimhan, B., Kato, T., Somura, H., Watanabe, H., Eguchi, S., Cui, Y., Sakaguchi, A., Tu, L.H., Jiang, R., Kim, M.-K., Arnold, J.G., Ouyang, W., 2022. Simulation of rice paddy systems in SWAT: a review of previous applications and proposed SWAT+ rice paddy module. Int. J. Agric. Biol. Eng. 15 (1), 1–24. https://doi.org/10.25165/j.ijabe.20221501.7147.

Gupta, H.V., Kling, H., Yilmaz, K.K., Martinez, G.F., 2009. Decomposition of the mean squared error and NSE performance criteria: implications for improving hydrological modelling. J. Hydrol. 377, 80–91. https://doi.org/10.1016/j.jhydrol.2009.08.003.

Hunt, N.D., Hill, J.D., Liebman, M., 2019. Cropping system diversity effects on nutrient discharge, soil erosion, and agronomic performance. Environ. Sci. Technol. 53, 1344–1352. https://doi.org/10.1021/acs.est.8b02193.

Hydrologic and Water Quality System (HAWQS), 2020. A National Watershed and Water Quality Assessment Tool; U.S. Environmental Protection Agency, Washington, DC, USA Available online https://epahawqs.tamu.edu.

Ikenberry, C.D., Soupir, M.L., Helmers, M.J., Crumpton, W.G., Arnold, J.G., Gassman, P.W., 2017. Simulation of daily flow pathways, tile-drain nitrate concentrations, and soil-nitrogen dynamics using SWAT. J. Am. Water Resour. Assoc. 53, 1251–1266. https://doi.org/10.1111/1752-1688.12569.

ISU, 2018. Nitrogen use in Iowa corn production. Crop 3073 (Revised). Iowa State University Extension and Outreach, Ames, IA . https://store.extension.iastate.edu/product/14281.

Jones, C.S., Nielsen, J.K., Schilling, K.E., Weber, L.J., 2018. Iowa stream nitrate and the Gulf of Mexico. PLoS One 13 (4), e0195930. https://doi.org/10.1371/journal.pone.0195930.

Kannan, N., Santhi, C., Williams, J.R., Arnold, J.G., 2008. Development of a continuous soil moisture accounting procedure for curve number methodology and its behavior with different evapotranspiration methods. Hydrol. Process. 22 (13), 2114–2121. https://doi.org/10.1002/hyp.6811.

Kleinman, P.J.A., Smith, D.R., Bolster, C.H., Easton, Z.M., 2015. Phosphorus fate, management, and modeling in artificially drained systems. J. Environ. Qual. 44 (2), 460–466. https://doi.org/10.2134/jeq2015.02.0090.

Kling, C.L., Arritt, R.W., Calhoun, G., Keiser, D.A., 2017. Integrated assessment models of the food, energy, and water nexus: a review and an outline of research needs. Ann. Rev. Resour. Econ. 9 (2017), 143–163. https://doi.org/10.1146/annurev-resource-100516-033533.

Lim, K.J., Engel, B.A., Tang, Z., Choi, J., 2005. Automated web GIS based hydrograph analysis tool. WHAT. J. Am. Water Resour. Assoc. 1397, 1407–1416.

McCallum, I., Montzka, C., Bayat, B., Kollet, S., Kolotii, A., Kussul, N., Lavreniuk, M., Lehmann, A., Maso, J., Mazzetti, P., Mosnier, A., Perracchione, E., Putth, M., Santoro, M., Serral, I., Shumilo, L., Spengler, D., Fritz, S., 2020. Developing food, water and energy nexus workflows. Int. J. Dig. Earth. 13 (2), 299–308. https://doi.org/10.1080/17538947.2019.1626921.

Miller, B.A., Crumpton, W.G., van der Valk, A.G., 2009. Spatial distribution of historical wetland classes on the DesMoines Lobe, Iowa. Wetlands 29 (4), 1146–1152. https://doi.org/10.1672/08-158.1.

Moriasi, D., Wilson, B., 2012. Hydrologic and water quality models: use, calibration, and validation. Am. Soc. Agric. Biol. Eng. 55, 1241–1247. https://doi.org/10.13031/2013.42265.

Moriasi, D.N., Arnold, J.G., Van Liew, M.W., Binger, R.L., Harmel, R.D., Veith, T.L., 2007. Model evaluation guidelines for systematic quantification of accuracy in watershed simulations. Trans. ASABE 50, 885–900. https://doi.org/10.13031/2013.23153.

Moriasi, D.N., Rossi, C.G., Arnold, J.G., Tomer, M.D., 2012. Evaluating hydrology of the Soil and Water Assessment Tool (SWAT) with new tile drain equations. J. Soil Water Conserv. 67, 513–524. https://doi.org/10.2489/jswc.67.6.513.

Moriasi, D.N., Gowda, P.H., Arnold, J.G., Mulla, D.J., Ale, S., Steiner, J.L., Tomer, M.D., 2013. Evaluation of the Hooghoudt and Kirkham tile drain equations in the Soil and Water Assessment Tool to simulate tile flow and nitrate-nitrogen. J. Environ. Qual. 42, 1699–1710. https://doi.org/10.2134/jeq2013.01.0018.

Moriasi, D.N., Gitau, M.W., Pai, N., Daggupati, P., 2015. Hydrologic and water quality models: performance measures and evaluation criteria. Trans. ASABE 58, 1763–1785. https://doi.org/10.13031/trans.58.10715.

Moussa, R., Chahinian, N., Bocquillon, C., 2007. Distributed hydrological modelling of a Mediterranean mountainous catchment - model construction and multi-site validation. J. Hydrol. 337, 35–51. https://doi.org/10.1016/j.jhydrol.2007.01.028.

Nair, S.S., King, K.W., Witter, J.D., Sohngen, B.L., Fausey, N.R., 2011. Importance of crop yield in calibrating watershed water quality simulation tools. J. Am. Water Resour. Assoc. 47 (6), 1285–1297.

Neitsch, S., Arnold, J., Kiniry, J., Williams, J., 2011. Soil & water assessment tool theoretical documentation version 2009. Texas Water Resour. Inst., 1–647 https://doi.org/10.1016/j.scitotenv.2015.11.063.

Patil, S.D., Stieglitz, M., 2015. Comparing spatial and temporal transferability of hydrological model parameters. J. Hydrol. 525, 409–417. https://doi.org/10.1016/j.jhydrol.2015.04.003.

Peel, M.C., Finlayson, L.B., McMahon, T.A., 2007. Updated world map of the KÖppen-Geiger climate classificatio. Hydrol. Earth Syst. Sci. 11, 1633–1644. https://doi.org/10.1002/ppp.421.

PRISM Climate Group, 2022. PRISM climate data. Parameter-Elevation Relationships on Independent Slopes Model (PRISM), Northwest Alliance for Computational Science and Engineering. Oregon State University, Corvallis, OR . https://www.prism.oregonstate.edu/.

Prokopy, L.S., Gramig, B.M., Bower, A., Church, S.P., Ellison, B., Gassman, P.W., Genskow, K., Gucker, D., Hallett, S.G., Hill, J., Hunt, N., Johnson, K.A., Kaplan, I., Kelleher, J.P., Kok, H., Komp, M., Lammers, P., LaRose, S., Liebman, M., Margenot, A., Mulla, D., O'Donnell, M.J., Peimer, A.W., Reaves, E., Salazar, K., Schelly, C., Schilling, K., Secchi, S., Spaulding, A.D., Swenson, D., Thompson, A.W., Ulrich-Schad, J.D., 2020. The urgency of transforming the Midwestern U.S. landscape into more than corn and soybean. Agric. Hum. Values 37, 537–539. https://doi.org/10.1007/s10460-020-10077-x.

Quade, D.J., Giglierano, J.D., Bettis III, E.A., Wisner, R.J, 2001. Overview of the Surficial Geologic Map of the Des Moines Lobe of Iowa, Phase 3: Boone and Story counties, scale 1:100,000. Iowa Department of Natural Resource.

Rossi, C.G., Srinivasan, R., Jirayoot, K., Le Duc, T., Souvannabouth, P., Binh, N., Gassman, P.W., 2009. Hydrologic evaluation of the lower Mekong River Basin with the Soil and Water Assessment Tool model. Int. Agric. Eng. J. 18, 1–13.

Schilling, K.E., Wolter, C.F., 2009. Modeling nitrate-nitrogen load reduction strategies for the Des Moines River, Iowa using SWAT. Environ. Manag. 44 (4), 671–682. https://doi.org/10.1007/s00267-009-9364-y.

Schilling, K.E., Gassman, P.W., Arenas-Amado, A., Jones, C.S., Arnold, J., 2019. Quantifying the contribution of tile drainage to basin-scale water yield using analytical and numerical models. Sci. Total Environ. 657, 297–309. https://doi.org/10.1016/j.scitotenv.2018.11.340.

Schilling, K.E., Langel, R.J., Wolter, C.F., Arenas-Amado, A., 2021. Using baseflow to quantify diffuse groundwater recharge and drought at a regional scale. J. Hydrol. 602, 126765. https://doi.org/10.1016/j.jhydrol.2021.126765.

Schull, V.Z., Daher, B., Gitau, M.W., Mehan, S., Flanagan, D.C., 2020. Analyzing FEW nexus modeling tools for water resources decision-making and management applications. Food Bioprod. Process. 119, 108–124. https://doi.org/10.1016/j.fbp.2019.10.011.

Seibert, J., McDonnell, J.J., 2002. On the dialog between experimentalist and modeler in catchment hydrology: use of soft data for multicriteria model calibration. Water Resour. Res. 38. https://doi.org/10.1029/2001wr000978 23-1-23–14.

Skaggs, R.W., Youssef, M.A., Chescheir, G.M., 2012. DRAINMOD: model use, calibration and validation. Trans. ASABE 55 (4), 1509–1522. https://doi.org/10.13031/2013.42259.

Sprague, L.A., Hirsch, R.M., Aulenbach, B.T., 2011. Nitrate in the Mississippi River and its tributaries, 1980 to 2008: are we making progress? Environ. Sci. Technol. 45 (17), 7209–7216. https://doi.org/10.1021/es201221s.

Stone, T.F., Thompson, J.R., Rosentrater, K.A., 2021. A Life Cycle assessment approach for vegetables in large-, mid-, and small-scale food systems in the Midwest US. Sustainability 13.

Tan, M.L., Gassman, P.W., Srinivasan, R., Arnold, J.G., Yang, X.Y., 2019. A review of SWAT studies in Southeast Asia: applications, challenges and future directions. Water (Switzerland) 11, 1–25. https://doi.org/10.3390/w11050914.

Tan, M.-L., Gassman, P., Yang, X., Haywood, J., 2020. A review of SWAT applications, performance and future needs for simulation of hydro-climatic extremes. Adv. Water Resour. 143, 103662. https://doi.org/10.1016/j.advwatres.2020.103662.

Texas A&M, 2017. HAWQS v1.0: Inputs. Spatial Sciences Laboratory, Texas A&M AgriLife Research, College Station, TX and Office of Water, Immediate Office, U.S. Environmental Protection Agency, Washington, DC. https://hawqs.tamu.edu/#/help.

Texas A&M, 2019. HAWQS User Guide. Version 1.1. Spatial Sciences Laboratory, Texas A&M AgriLife Research, College Station, TX and Office of Water, Immediate Office, U.S. Environmental Protection Agency, Washington, DC. https://hawqs.tamu.edu/#/help.

Thompson, J., Ganapathysubramanian, B., Chen, W., Dorneich, M., Gassman, P., Krejci, C., Liebman, M., Nair, A., Passe, U., Schwab, N., Rosentrater, K., Stone, T., Wang, Y., Zhou, Y., 2021. Iowa Urban FEWS: integrating social and biophysical models for exploration of urban food, energy, and water systems. Front. Big Data 4, 1–18. https://doi.org/10.3389/fdata.2021.662186.

USDA-NASS, 2022. Research and Science: CropScape and Cropland Data Layer - National Download. U.S.

USDA-NRCS, 2004. Part 630: Hydrology. Chapter 10: Estimation of Direct Runoff from Storm Rainfall: Hydraulics and Hydrology: Technical References. NRCS National Engineering Handbook. U.S. Department of Agriculture. http://www.nrcs.usda.gov/wps/portal/nrcs/detailfull/national/water/?cid=stelprdb1043063.

USDA-NRCS, 2021. Soil Orders Map of the United States. USDA. https://www.nrcs.usda.gov/wps/portal/nrcs/main/soils/survey/class/maps/.

USDA-NRCS, 2022a. Description of SSURGO Database. U.S. Department of Agriculture, Natural Resources Conservation Service, Washington, D.C. https://www.nrcs.usda.gov/wps/portal/nrcs/detail/soils/survey/?cid=nrcs142p2_053627.

USDA-NRCS, 2022b. Description of STATSGO2 Database. U.S. Department of Agriculture, Natural Resources Conservation Service, Washington, D.C. https://www.nrcs.usda.gov/wps/portal/nrcs/detail/soils/survey/geo/?cid=nrcs142p2_053629.

USDA-NRCS, 2022c. Soil Data Access: Query Services for Custom Access to Soil Data. U.S. Department of Agriculture, Natural Resources Conservation Service, Washington, D.C. https://sdmdataaccess.nrcs.usda.gov/.

USEPA, 2019. HAWQS User Guide. Available online at https://hawqs.tamu.edu/content/docs/HAWQS-User-Guide.pdf.

USGS, 2013. Federal standards and procedures for the National Watershed Boundary Dataset (WBD). Techniques and Methods 11-A3, Chapter 3 of Section A, Federal Standards Book 11, Collection and Delineation of Spatial Data, fourth ed U.S. Department of the Interior, U.S. Geological Survey, Reston, VA and U.S. Department of Agriculture, Natural Resources Conservation Service, Washington, DC . http://pubs.usgs.gov/tm/tm11a3/.

USGS, 2018. National Land Cover Database. U.S. Geological Survey, Earth Resources Observation and Science (EROS) Center, Sioux Falls, SD. https://www.usgs.gov/centers/eros/science/national-land-cover-database.

USGS, 2022. Hydrologic Unit Codes (HUCs) Explained. Accessed by: https://nas.er.usgs.gov/hucs.aspx.

Valayamkunnath, P., Barlage, M., Chen, F., Gochis, D.J., Franz, K.J., 2020. Mapping of 30-meter resolution tile-drained croplands using a geospatial modeling approach. Sci. Data 7, 1–10. https://doi.org/10.1038/s41597-020-00596-x.

White, M., Gambone, M., Yen, H., Daggupati, P., Bieger, K., Deb, D., Arnold, J., 2016. Development of a cropland management dataset to support U.S. swat assessments. J. Am. Water Resour. Assoc. 52 (1), 269–274. https://doi.org/10.1111/1752-1688.12384.

Williams, J.R., Kannan, N., Wang, X., Santhi, C., Arnold, J.G., 2012. Evolution of the SCS runoff curve number method and its application to continuous runoff simulation. J. Hydrol. Eng. 17 (11), 1221–1229. https://doi.org/10.1061/(ASCE)HE.1943-5584.0000529.

Wright, C.K., Wimberly, M.C., 2013. Recent land use change in the western corn belt threatens grasslands and wetlands. Proc. Natl. Acad. Sci. U. S. A. 110, 4134–4139. https://doi.org/10.1073/pnas.1215404110.

Yang, X., Liu, Q., Fu, G., He, Y., Luo, X., Zheng, Z., 2016. Spatiotemporal Patterns and Source Attribution of Nitrogen Load in a River Basin With Complex Pollution Sources. 94 pp. 187–199.